

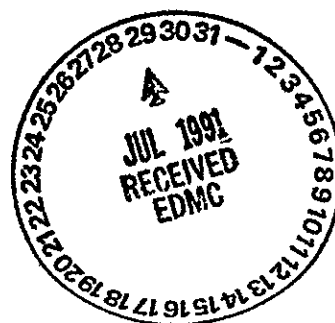
START

WHC-SD-ER-TA-001

Numerical Simulation of Strontium-90 Transport from the 100-N Area Liquid Waste Disposal Facilities

M. P. Connelly
J. D. Davis
P. D. Rittmann

Date Published
February 1991



Prepared for the U.S. Department of Energy
Office of Environmental Restoration and
Waste Management



**Westinghouse
Hanford Company**

P.O. Box 1970
Richland, Washington 99352

Hanford Operations and Engineering Contractor for the
U.S. Department of Energy under Contract DE-AC06-87RL10930

9513381.0003

WHC-SD-ER-TA-001

ACKNOWLEDGEMENTS

This work was funded by the U.S. Department of Energy through the Environmental Safety Program at Westinghouse Hanford Company. Completion of the analysis would not have been possible without the support of K. A. Gano, Manager of Environmental Protection; D. J. Watson, Manager of Environmental Safety; and G. S. Hunacek, Jr., Project Manager.

9513381.0004

WHC-SD-ER-TA-001

This page intentionally left blank.

9513381.0005

WHC-SD-ER-TA-001

ACKNOWLEDGEMENTS

This work was funded by the U.S. Department of Energy through the Environmental Safety Program at Westinghouse Hanford Company. Completion of the analysis would not have been possible without the support of K. A. Gano, Manager of Environmental Protection; D. J. Watson, Manager of Environmental Safety; and G. S. Hunacek, Jr., Project Manager.

9513381.0006

WHC-SD-ER-TA-001

This page intentionally left blank.

NUMERICAL SIMULATION OF STRONTIUM-90 TRANSPORT
FROM THE 100-N AREA LIQUID WASTE
DISPOSAL FACILITIES

M. P. Connelly
J. D. Davis
P. D. Rittmann

ABSTRACT

This report describes an analysis of groundwater movement and transport of strontium-90 in groundwater from the 100-N Area liquid waste disposal facilities to the Columbia River. To provide a perspective on the potential effects of discharges of groundwater contaminated by strontium-90 to the Columbia River, the analysis included estimates of maximum radiation doses to humans that could result if no remedial actions were taken. The objectives of the analysis were to help define the need for additional data and to predict the future effects of the facilities on the groundwater quality at the shoreline of the Columbia River adjoining the 100-N Area, given the cessation of effluent discharges to the facilities.

9513381.0008

WHC-SD-ER-TA-001

This page intentionally left blank.

PREFACE

This groundwater and contaminant migration study was performed to assess the releases of strontium-90 to the Columbia River given the significant reduction in liquid effluent disposal practices to the soil column. This assessment is being made with regards to compliance to U.S. Department of Energy Order 5400.5, "Radiation Protection of the Public and Environment." As such, the report assesses the releases of strontium-90 to the Columbia River from the 100-N Area in the absence of any mitigative actions. In addition, the report helps to support ongoing environmental monitoring associated with 100-N Area operations. Hence, the assessment evaluates the potential offsite dose from releases of strontium-90 to the Columbia River at the N Springs seepages bordering the 100-N Area.

This report provides a more detailed assessment of groundwater and contaminant migration potential of that which is described in the *Liquid Effluent Study Project Plan* (Rohay 1990).

Methods to mitigate current and projected future releases of strontium-90 will be addressed in a subsequent study beginning in fiscal year (FY) 1991. The results reported in this document and those from the subsequent evaluation will be used to help determine the future course of action in minimizing the releases of strontium-90 to the environment.

9513381.0010

WHC-SD-ER-TA-001

This page intentionally left blank.

CONTENTS

| | | |
|-------|--|----|
| 1.0 | INTRODUCTION | 1 |
| 1.1 | LIQUID WASTE DISPOSAL FACILITY DESCRIPTION AND HISTORY | 1 |
| 1.2 | DESCRIPTION OF PROBLEM | 8 |
| 1.3 | OBJECTIVE | 9 |
| 1.4 | SCOPE | 9 |
| 2.0 | GENERAL APPROACH | 11 |
| 3.0 | GEOLOGY | 15 |
| 3.1 | RINGOLD FORMATION | 15 |
| 3.2 | HANFORD FORMATION | 15 |
| 4.0 | MODEL DESCRIPTION | 17 |
| 4.1 | GEOMETRY | 17 |
| 4.2 | SOURCE TERMS | 17 |
| 4.3 | BOUNDARY CONDITIONS | 20 |
| 4.4 | NUMERICAL DISCRETIZATION | 23 |
| 4.5 | HYDROLOGIC PROPERTIES | 23 |
| 4.5.1 | Soil Moisture Characteristics | 23 |
| 4.5.2 | Saturated Hydraulic Conductivity | 27 |
| 4.5.3 | Effective Porosity and Volumetric Moisture Content | 32 |
| 4.6 | TRANSPORT PROPERTIES | 33 |
| 5.0 | MODEL CALIBRATION | 35 |
| 5.1 | CALIBRATION OF THE GROUNDWATER FLOW EQUATION | 35 |
| 5.2 | CALIBRATION OF THE CONTAMINANT TRANSPORT EQUATION FOR ^{90}Sr . . | 39 |
| 6.0 | RESULTS OF THE GROUNDWATER FLOW AND CONTAMINANT TRANSPORT ANALYSES | 41 |
| 6.1 | GROUNDWATER FLOW | 41 |
| 6.2 | CONTAMINANT TRANSPORT | 45 |
| 7.0 | RADIATION DOSE FROM ^{90}Sr RELEASED FROM THE 100-N AREA LWDFs THAT ENTERS THE COLUMBIA RIVER AT N SPRINGS | 49 |
| 7.1 | ANNUAL RATE OF ^{90}Sr DISCHARGE TO THE COLUMBIA RIVER | 49 |
| 7.2 | The ^{90}Sr PATHWAYS TO HUMAN | 49 |
| 7.3 | DATA FILES USED BY GENII | 52 |
| 7.4 | COMPUTATION OF CUMULATIVE RADIATION COMMITMENTS | 52 |
| 8.0 | SUMMARY AND RECOMMENDATIONS | 61 |
| 9.0 | REFERENCES | 63 |

FIGURES

| | | |
|----|---|----|
| 1 | Location of the Liquid Waste Disposal Facilities in the 100-N Area . | 2 |
| 2 | Layout of the 1324-N/NA Liquid Waste Disposal Facility | 3 |
| 3 | Layout of the 1301-N Liquid Waste Disposal Facility | 5 |
| 4 | Layout of the 1325-N Liquid Waste Disposal Facility | 7 |
| 5 | Ten Data-Collection Sites Down-Gradient from the 100-N Area LWDFs . | 12 |
| 6 | Near-Surface Hydrogeologic Units in the 100-N Area | 16 |
| 7 | Conceptual Model for the Numerical Simulation for the 100-N Area N Springs Project | 18 |
| 8 | Geologic Cross Section of the 100-N Area | 19 |
| 9 | Average Effluent Flows and ⁹⁰ Sr Concentrations Received by the 1301-N, 1324-N-NA, and 1325-N Liquid Waste Disposal Facilities . . . | 22 |
| 10 | Numerical Grid Used in the 100-N Area Simulation | 25 |
| 11 | Comparison of Moisture Characteristic Data from the Field with Fitted Moisture Characteristics Curves Using Van Genuchten RETC Program | 28 |
| 12 | Relative Hydraulic Conductivities as a Function of Matrix Potential for the 10 Sites | 29 |
| 13 | Moisture Characteristic Curves Showing Relative Hydraulic Conductivities and Matrix Potential as a Function of Volumetric Water Content | 29 |
| 14 | Calculated Arrival Times of a Nonsorbed Solute. The decrease in concentration at 1.25 yr is due to a higher elevation of the Columbia River | 36 |
| 15 | Observed Water Table Elevations in July 1969 | 37 |
| 16 | Water Table Elevations Simulated by PORFLO for July 1969 | 38 |
| 17 | Observed Concentrations of ⁹⁰ Sr at the 1301-N LWDF and N Springs . . | 40 |
| 18 | Observed and Simulated Peak Concentrations of ⁹⁰ Sr at N Springs . . | 40 |
| 19 | Selected PORFLO-3 Results Showing the Initial Conditions and the Rise in the Water Table Beneath the 1301-N Liquid Waste Disposal Facility | 42 |

FIGURES (continued)

| | | |
|----|--|----|
| 20 | Selected PORFLO-3 Results Showing the Development of Steady-State Groundwater Flow Conditions Beneath the 1301-N Liquid Waste Disposal Facility | 43 |
| 21 | Selected PORFLO-3 Results Showing the Perturbation of Steady-State Conditions Caused by Effluent Discharges to the 1324-N/NA and 1325-N Liquid Waste Disposal Facility (21a through 21c) and the Interaction of the Columbia River with the Unconfined Aquifer (21d through 21f) | 44 |
| 22 | Selected Time-Dependent PORFLO-3 Results Showing the Downward and Outward Growth of the ^{90}Sr Plume Beneath the 1301-N Liquid Waste Disposal Facility | 46 |
| 23 | Selected Time-Dependent PORFLO-3 Results Showing the Areal Extent of the ^{90}Sr Plume in the Unconfined Aquifer | 48 |
| 24 | Comparison Between Annual Discharges of ^{90}Sr Calculated by PROFLO-3 to Reported Discharges for the Years 1973 Through 1989 | 51 |
| 25 | Comparison of Effective Dose Equivalents Generated by GENII and the Curve-Fitting Equation | 54 |
| 26 | Comparison of Bone Dose Calculated Using GENII and the Curve-Fitting Equation | 54 |
| 27 | Annual and Cumulative Releases of ^{90}Sr from the 100-N Area Liquid Waste Disposal Facility to the Columbia River | 57 |
| 28 | Annual and Cumulative Doses from ^{90}Sr Released from the 100-N Area Liquid Waste Disposal Facility | 57 |
| 29 | The Effect of Residual Contamination on Computation of Annual Exposures | 59 |
| 30 | The Effect of Residual Contamination of Cumulative Exposures | 59 |

TABLES

| | | |
|---|---|---|
| 1 | Approximate Discharge Rates and Characteristics of Effluents Discharged to the 1324-N/NA Liquid Waste Disposal Facility | 4 |
| 2 | Characteristics of the Principal Radionuclides in Effluents Discharged to the 1301-N Liquid Waste Disposal Facility | 6 |
| 3 | Characteristics of the Principal Radionuclides in Effluents Discharged to the 1325-N Liquid Waste Disposal Facility | 8 |

TABLES (continued)

| | | |
|----|---|----|
| 4 | Source-Term Values Assigned for the Numerical Model | 21 |
| 5 | Assigned Boundary Types and Values | 24 |
| 6 | Hydrologic and Transport Properties Used in the Simulation | 26 |
| 7 | Hydrologic Parameters Derived from Field Sites in the 100-N Area . . | 30 |
| 8 | Annual Discharges of ^{90}Sr to the Columbia River From the 100-N Area Liquid Waste Disposal Facilities Via N Springs Estimated by the PORFLO-3 Software | 50 |
| 9 | Comparison of GENII and Curve-Fitting Equation Results Cumulative Dose per Curie of ^{90}Sr Released | 53 |
| 10 | Seventy-Year Effective Dose Equivalent | 55 |
| 11 | Seventy-Year Dose to the Bone Surface | 56 |

NUMERICAL SIMULATION OF STRONTIUM-90 TRANSPORT
FROM THE 100-N AREA LIQUID WASTE
DISPOSAL FACILITIES

1.0 INTRODUCTION

Three facilities have been used for disposal of effluents from the start of operations at the N Reactor in 1963 to the present. The 1324 Neutralization Basin (1324-N) and Percolation Pond (1324-NA) were used to neutralize and dispose of nonradioactive, acidic, and caustic effluents from regeneration of ion-exchange-column resins. The 1301-N Liquid Waste Disposal Facility (LWDF) and 1325-N LWDF were used for disposal of effluents with low-level fission and activation products (Figure 1). The 1301-N and 1325-N LWDFs were designed to remove, by sorption, filtration, and ion exchange, a high percentage of radionuclides in the effluent.

The 1324-N/NA facility has been used since 1977. The 1301-N LWDF began operation in December 1963 and was retired from service in September 1985. Since then, the 1325-N LWDF has received essentially all of the radioactive liquid effluents discharged in the 100-N Area.

The operation of these three facilities resulted in perturbation of the groundwater in the 100-N Area, including a rise in the elevation of the water table beneath all three facilities and the development of plumes of radioactively contaminated groundwater emanating from the 1301-N and 1325-N LWDFs. With the cessation of reactor operation and many related activities in the 100-N Area in 1987, these sources of recharge to the unconfined aquifer have been significantly reduced and will cease to exist by 1995. Whether the discharge of groundwater containing strontium-90 (^{90}Sr) to the Columbia River via riverbank seepage (N Springs) caused by disposal of the effluent is likely to abate or end with the termination of LWDF operations is the topic of this report.

1.1 LIQUID WASTE DISPOSAL FACILITY DESCRIPTION AND HISTORY

The 1324-N Surface Impoundment Basin and 1324-NA Percolation Pond are used to neutralize and dispose of effluents from the 163-N Demineralization Plant. The 1324-N basin (Figure 2) is a 22.9-m-long-by 42.7-m-wide-by 4.6-m-deep-rectangular basin. Its sloping sides and bottom are covered by two impervious liners. The facility has operated intermittently; effluents were discharged to the pond for adjustment of their pH to between 4.0 and 11.0. These discharges averaged 1,700,000 L/d. After pH adjustment, the effluents from 1324-N were discharged to the unlined 1324-NA pond for infiltration into the soil. Information on the quantity of effluent discharged to the 1324-NA pond is summarized in Table 1.

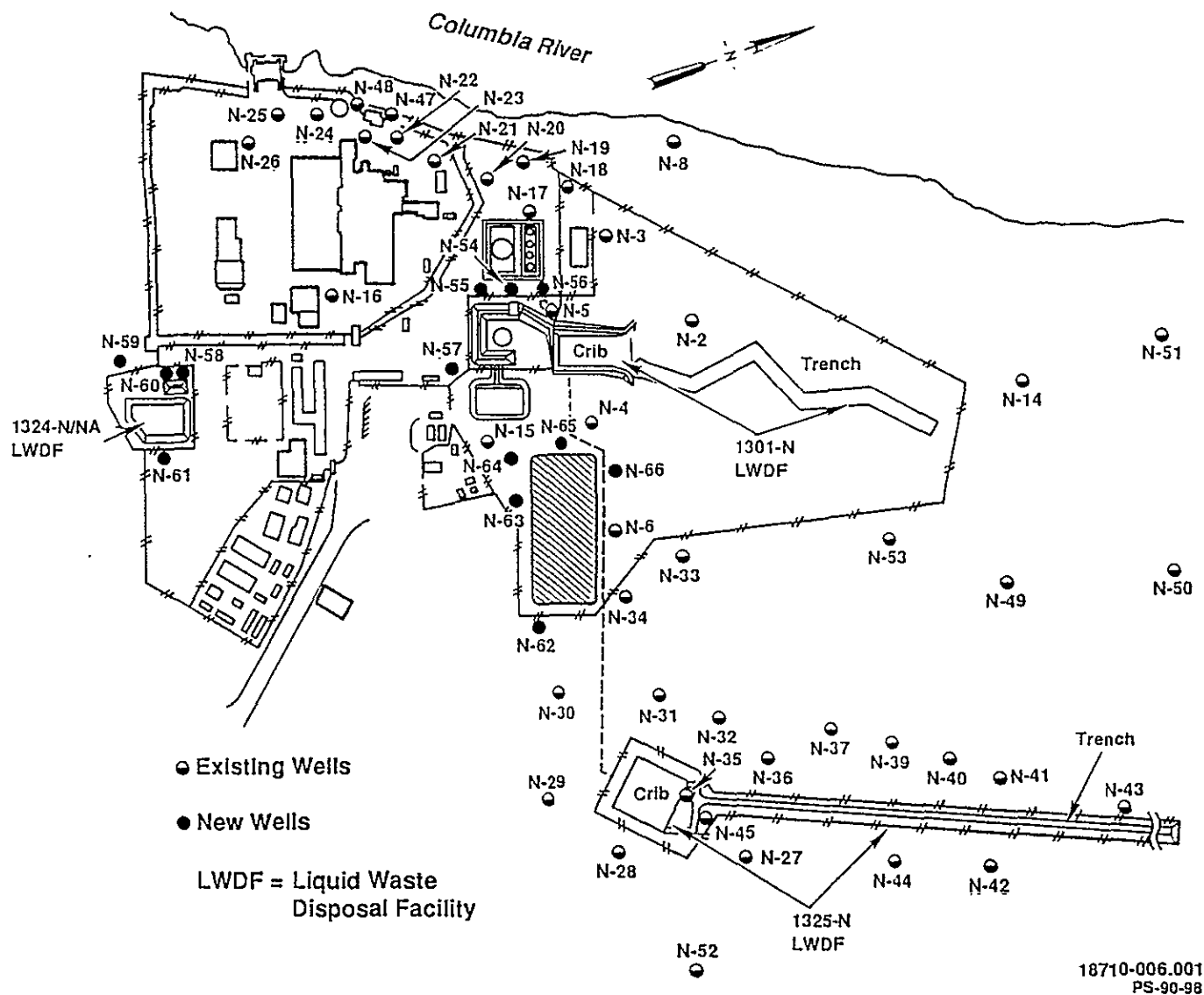


Figure 1. Location of the Liquid Waste Disposal Facilities in the 100-N Area.

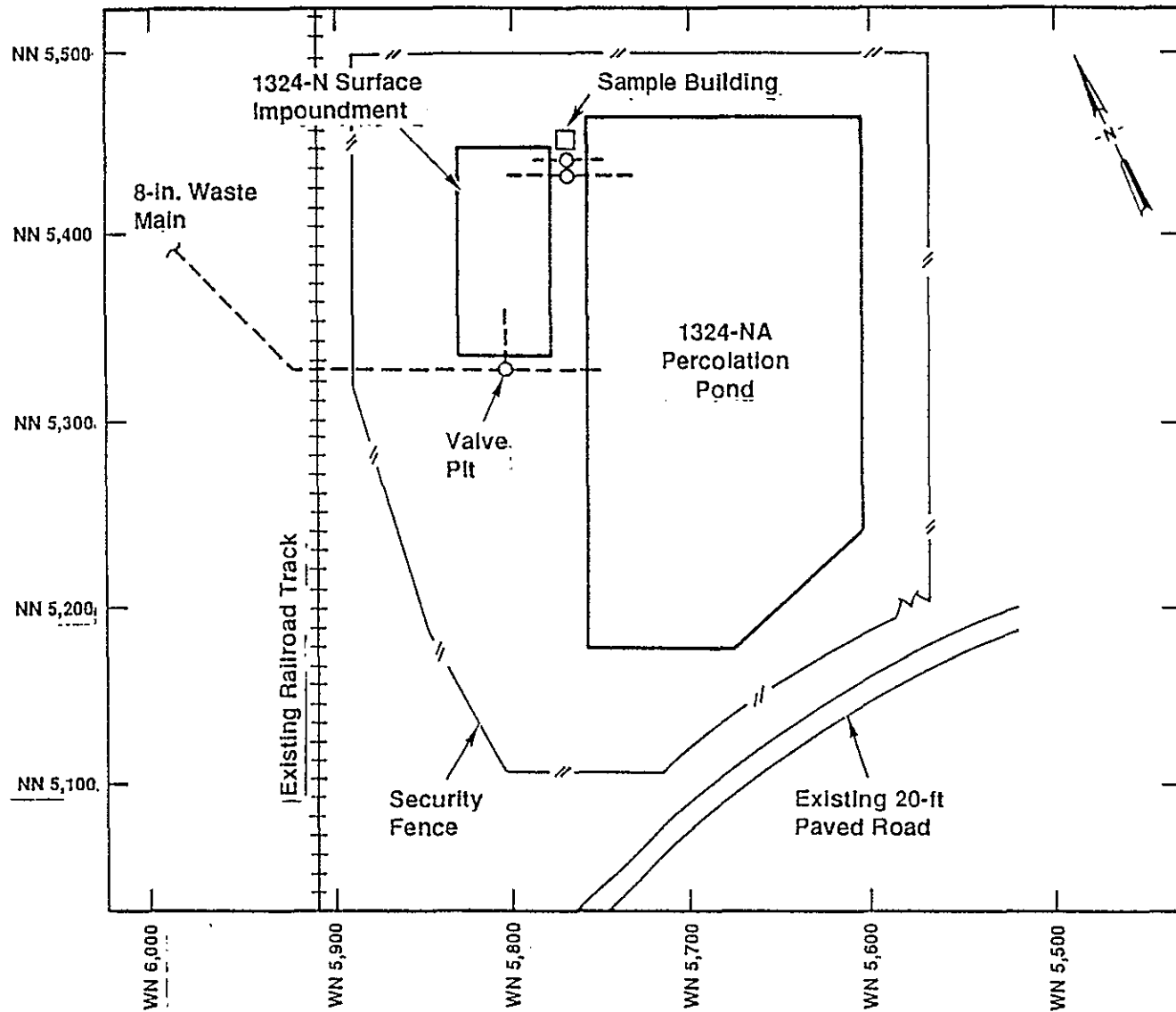


Figure 2. Layout of the 1324-N/NA Liquid Waste Disposal Facility.

Table 1. Approximate Discharge Rates and Characteristics of Effluents Discharged to the 1324-N/NA Liquid Waste Disposal Facility.

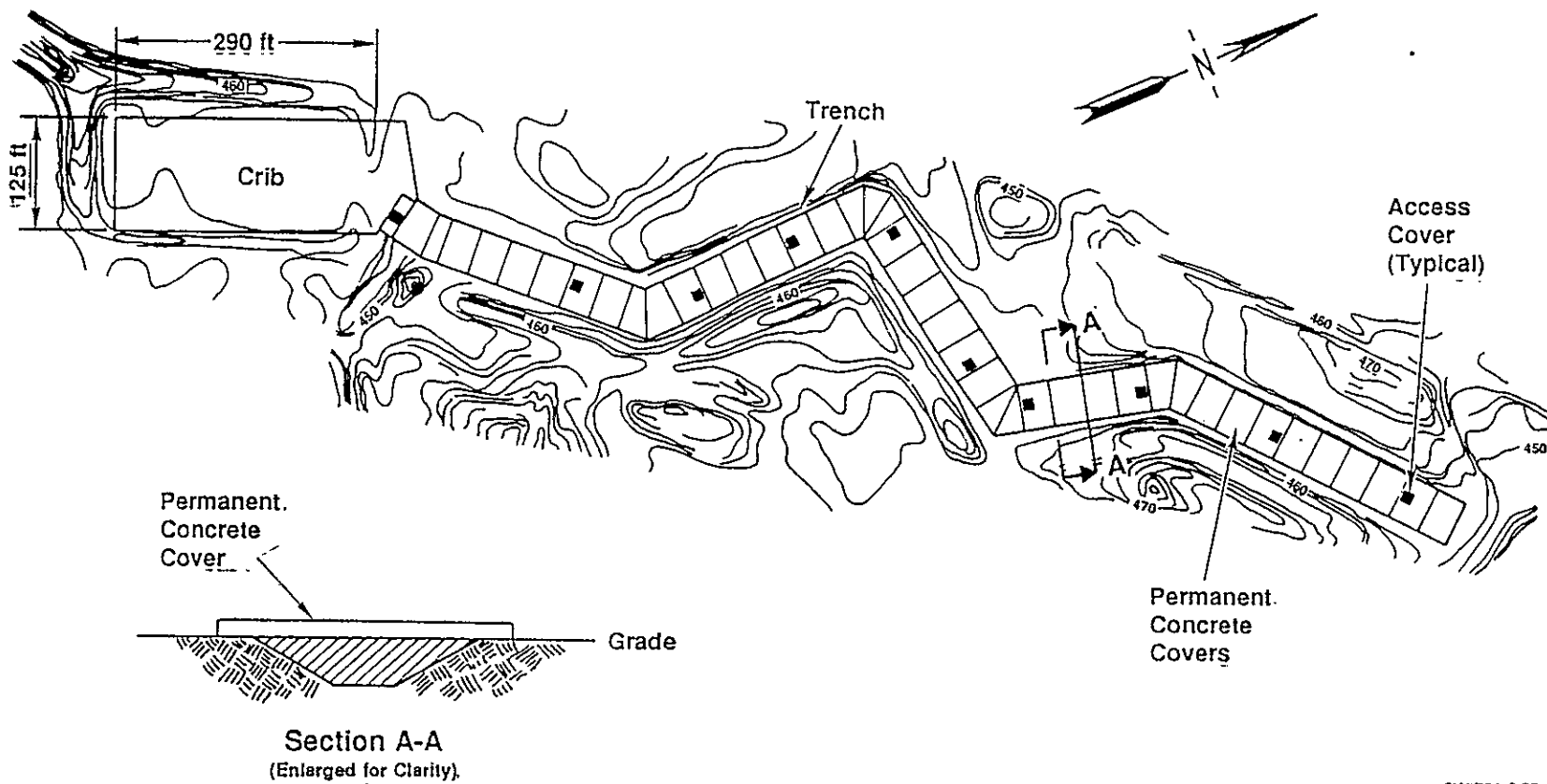
| Effluent source | Flow rate (L/m) |
|------------------------------------|------------------|
| Process cooling water | 940 |
| Acidic ion-exchange column wastes | 940 (for 30 m/d) |
| Caustic ion-exchange column wastes | 115 (for 70 m/d) |

Until September 1985, the 1301-N LWDF (Figure 3) was the principal means for disposal of N Reactor effluent containing low-level radioactivity. The average rate of effluent flow into this facility was 7,900 L/m. The rate of discharge varied widely in response to the operational status of the N Reactor. Liquid effluents came from the reactor and peripheral facility cooling systems, spent-fuel storage basin, and various drainage systems. The radioactivity entering the groundwater is primarily from ^3H and ^{90}Sr , with traces from ^{60}Co , ^{103}Ru , ^{106}Ru , ^{125}Sb , and ^{129}I . The major source of ^{90}Sr was ruptured, irradiated fuel elements that were stored in the water-filled 1324-N basin. The characteristics of the effluent discharged to the 1301-N LWDF are summarized in Table 2.

The bottom of the 1301-N LWDF is 18.3 m above the mean surface elevation of the Columbia River and 262.1 m from the shoreline. Liquid effluent streams were discharged at an average rate of 7,900 L/m into a 15.8-m-long-by-3.7-m-wide concrete weir box that empties into a rectangular basin (termed a "crib") measuring 88.4 m long by 38.1 m wide. This crib was constructed by excavating the soil and covering the bottom of the excavation with a 0.91-m-thick layer of riprap to facilitate percolation. An extension trench was later added to the crib in 1965. The crib extension is a ditch approximately 487.7 m long by 15.2 m wide by 3.7 m deep that was excavated in a zigzag configuration (Figure 3) to avoid topographic highs. Both the crib and the trench are covered by concrete panels to inhibit access.

During 1982, routine sampling of monitoring wells and seepage springs on the bank of the Columbia River adjacent to the 100-N Area indicated increasing concentrations of radionuclides, principally ^3H and ^{90}Sr , reaching the river. In March of 1988, ^{90}Sr estimated to be in the riverbank seepages accounted for approximately 60% of the calculated offsite exposure to a hypothetical, maximally exposed member of the public that could be attributed to the Hanford Site.

Releases of ^{90}Sr to the Columbia River were calculated based on the assumption that 50% of the effluent released to the LWDFs eventually appears as discharge at N Springs. The releases calculated for N Springs were 4.0 Ci in 1983, 7.0 Ci in 1984, 8.4 Ci in 1985, 7.9 Ci in 1986, 2.4 Ci in 1987,



2K8701-6.33
PS-90-99

Figure 3. Layout of the 1301-N Liquid Waste Disposal Facility.

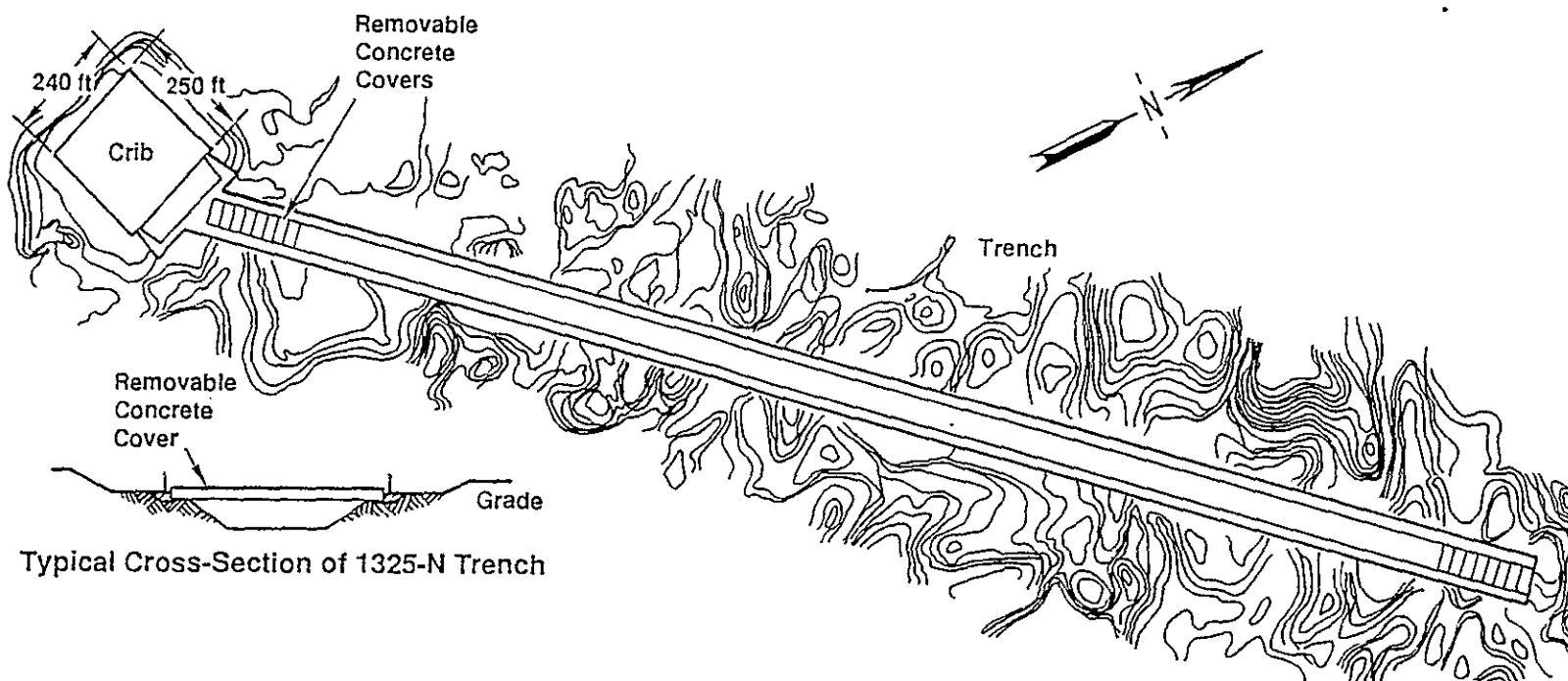
Table 2. Characteristics of the Principal Radionuclides in Effluents Discharged to the 1301-N Liquid Waste Disposal Facility.

| Cumulative Inventory as of January 1, 1988 | | |
|--|----------------|----------------|
| Radionuclide | Half-life (yr) | Inventory (Ci) |
| ^{60}Co | 5.3 | 2,300.0 |
| ^{90}Sr | 28.6 | 1,900.0 |
| ^{106}Ru | 1.0 | 3.7 |
| ^{134}Cs | 2.1 | 12.0 |
| ^{137}Cs | 30.0 | 2,600.0 |
| ^{239}Pu | 24,000.0 | 23.0 |

2.0 Ci in 1988, and 1.7 Ci in 1989 (Rokkan 1984, 1985, 1987, 1988; Perkins 1988, 1989). The occurrence of these releases at N Springs led to the hypothesis that, after 20 yr of operation, the ion-exchange, adsorption, and filtration capabilities of the soil underlying the 1301-N crib and trench had significantly diminished.

Consequently, the 1325-N crib (Figure 4) was constructed in October 1983 as a replacement for the 1301-N LWDF. This facility is 731.5 m from the Columbia River and is 73.2 m wide by 76.2 m long. After 2 yr of operation, during which the designed capacity of the crib was determined to be inadequate because of a rapid reduction in the percolation capacity of the soil, a 914.4-m-long, four-segment extension trench was excavated. The trench began service in September 1985 to augment the capacity of the crib. Both the crib and the trench are covered by concrete panels to inhibit access. The flow rate into the facility averaged 5,300 L/m from 1983 to 1986, 1,310 L/m in 1987, and less than 1,120 L/m since 1987. The constituents of the effluent discharged to the 1325-N LWDF and their inventories are summarized in Table 3.

Since September 1985, the 1301-N LWDF has not received significant quantities of effluent. Nevertheless, sufficient ^{90}Sr to be a concern has continued to reach the Columbia River. With the discontinuance of production at the N Reactor and mothballing of the facility in a dry lay-up status, discharges of effluent to the 1324-N/NA and 1325-N LWDFs have been reduced drastically and will cease by 1995. Hence, the mounding of the water table under the LWDFs will dissipate, and additional fluxes of water to the Columbia River from the LWDFs will cease.



2K8705-11.1
PS-90-100

Figure 4. Layout of the 1325-N Liquid Waste Disposal Facility.

Table 3. Characteristics of the Principal Radionuclides in Effluents Discharged to the 1325-N Liquid Waste Disposal Facility.

| Cumulative Inventory as of January 1, 1988 | | |
|--|----------------|----------------|
| Radionuclide | Half-life (yr) | Inventory (Ci) |
| ^{60}Co | 5.3 | 1,140.0 |
| ^{90}Sr | 28.6 | 210.0 |
| ^{106}Ru | 1.0 | 35.0 |
| ^{134}Cs | 2.1 | 10.0 |
| ^{137}Cs | 30.0 | 350.0 |
| ^{239}Pu | 24,000.0 | 2.0 |

Consequently, the factors affecting future groundwater flow and contaminant transport in the 100-N Area will be (1) the local geology, (2) the groundwater and soil chemistry, (3) the amount and flux of meteoric water available to recharge the water table, and (4) the influence of river level fluctuation on the elevation and flow vectors of the unconfined aquifer. These factors are considered by the analysis reported here.

1.2 DESCRIPTION OF PROBLEM

Monitoring of the fluctuation in elevation of the water table has confirmed that the recent large reduction of effluent discharges to the 1324-N/NA and 1325-N LWDFs has reduced the local perturbation of the natural groundwater flow system in the 100-N Area. The questions that remain are as follows:

- Will the cessation of liquid effluent discharges to the LWDFs in the 100-N Area stop or reduce the flux of ^{90}Sr entering the Columbia River to acceptably low levels (DOE Order 5400.5)?
- If the predicted flux exceeds levels deemed to be acceptable, what reduction of contaminant flux can be expected to be achieved by specific kinds of mitigative actions (subsequent report)?

1.3 OBJECTIVE

Finding defensible answers to these questions require (1) estimation of the future effects of the 100-N Area LWDFs on the water quality of the unconfined aquifer at the shoreline of the Columbia River bounding the 100-N Area, given the cessation of liquid effluent discharges to these facilities, (2) evaluation of the need for mitigative actions, and (3) estimates of the relative efficacy of potential mitigative actions, should such actions be needed. The work reported here attempts to answer only the first of these three questions.

1.4 SCOPE

The scope of work consisted of the following tasks:

- Assembling pertinent available information to formulate a conceptual model
- Obtaining new, site-specific information from field and laboratory measurements to refine the conceptual model
- Simulating past, present, and future groundwater flow and contaminant transport using the numerical methods of the VAM2DH* and PORFLO-3** computer software (Runchal and Sagar 1989, Sagar and Runchal 1989)
- Conducting sensitivity analyses to focus potential mitigative engineering efforts
- Formulating exposure scenarios and computing exposures
- Issuing a report describing the analysis and the results.

*VAM2DH is available on a proprietary basis from HydroGeologic, Inc., Herndon, Virginia.

**PORFLO-3 is available on a proprietary basis from Analytic and Computational Research, Inc., Los Angeles, California.

9513381.0024

WHC-SD-ER-TA-001

This page intentionally left blank.

2.0 GENERAL APPROACH

The work reported here was performed in accordance with Quality Assurance Program Requirements for Nuclear Facilities (ANSI/ASME NQA-1) and *Standard Engineering Practices* (WHC 1988).

The initial step in the analytical approach was to formulate a conceptual model of the shallow groundwater system and contaminant source. This conceptual model was used to determine what data were required for the numerical model. A search of published information was made to obtain readily available data. These data were used to define effluent volumes, and quantity of ^{90}Sr discharged to the LWDFs and detected in monitoring wells and riverbank seeps. Information on the local stratigraphy, unconfined aquifer characteristics, river-level fluctuations, precipitation, and near-surface water balance was used to define hydrogeologic conditions at the Hanford Site.

No information that met current quality assurance requirements was available on the soil moisture characteristics and hydraulic conductivities of sediments above the water table, downgradient from the LWDFs in the 100-N Area. Consequently, 10 sites appropriate for data collection were identified (Figure 5). At these locations, soil samples were collected for laboratory determination of moisture characteristic curves and soil pH. At the same locations, permeameters were installed to measure in situ hydraulic conductivities.

Two- and three-dimensional models of groundwater flow and contaminant transport in the vicinity of the 100-N Area LWDFs were numerically simulated using the VAM2DH and PORFLO-3 software. Both software packages comply with Westinghouse Hanford Company development and maintenance procedures for quality-affecting software; both have been widely used for groundwater flow and contaminant transport simulations at the Hanford Site.

A two-dimensional model of groundwater flow and contaminant transport was numerically simulated to compare the results with field measurements of past and present groundwater movement and contaminant flux (Lu 1990). Selected input parameters of the numerical model were adjusted until the results of the computer simulation closely matched those of the most recent field determinations of groundwater quality at N Springs. This simulation provided a baseline by which future changes could be evaluated.

After a reasonable match was achieved, the model was considered to approximate past and current conditions in the vicinity of the 100-N Area LWDFs. The duration of the simulation was extended to the year 2020 to predict future ^{90}Sr concentrations at N Springs, assuming the absence of future effluent discharges to the LWDFs. The results from this two-dimensional simulation were used to help define a three-dimensional model subsequently simulated by the PORFLO-3 software. A modeling process analogous to that used for the two-dimensional conceptual model was used to adjust the three-dimensional conceptual model simulated by PORFLO-3 before it was used to predict flow and transport 30 yr into the future.

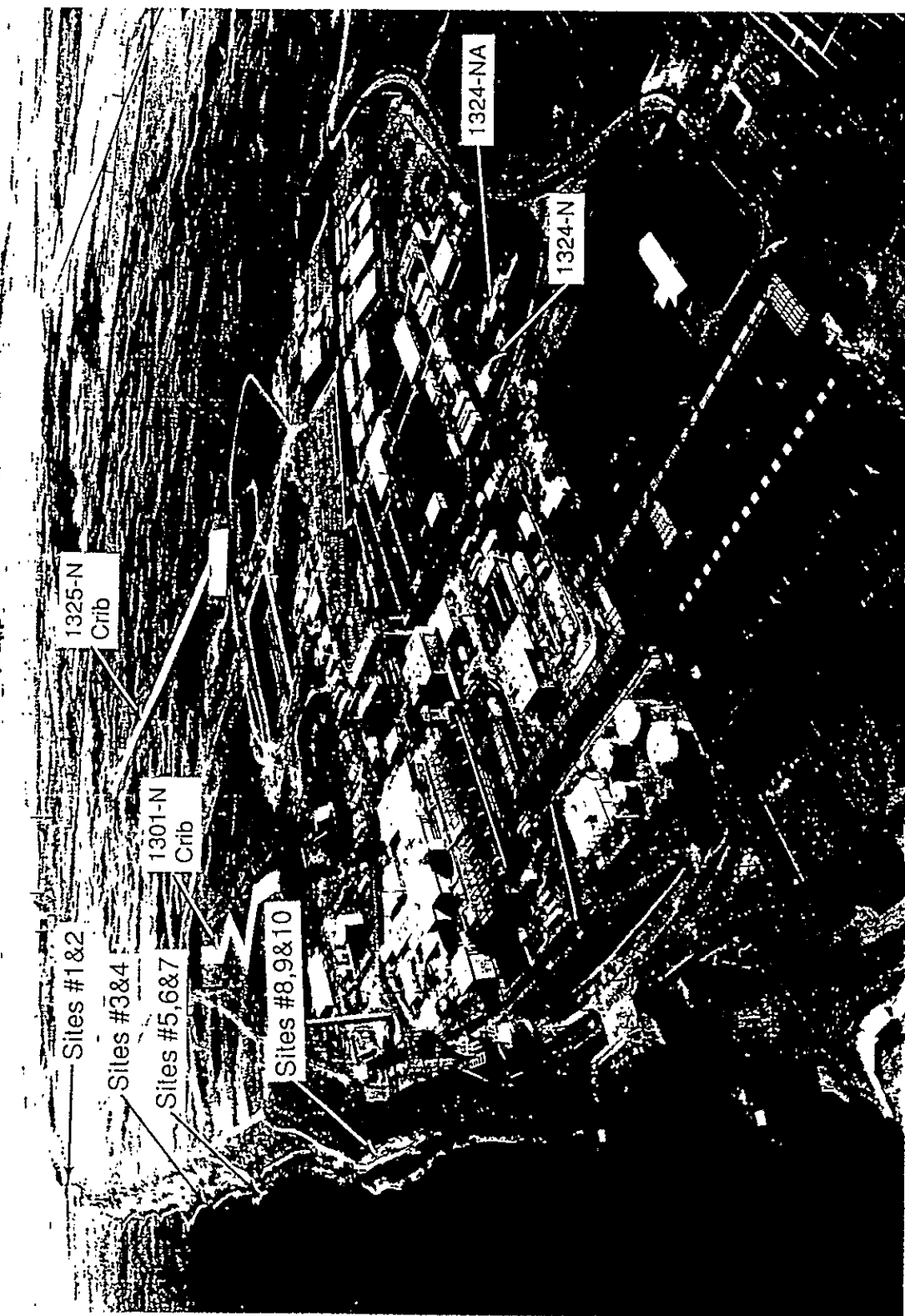


Figure 5. Ten Data-Collection Sites Down-Gradient from the 100-N Area Liquid Waste Disposal Facilities.

Results of the three-dimensional baseline and predictive simulations are reported in terms of (1) contaminant concentrations in soil moisture above the water table and in water of the unconfined aquifer, (2) streamlines, and (3) flow vectors.

9513381.0028

WHC-SD-ER-TA-001

This page intentionally left blank.

3.0 GEOLOGY

The geology of the suprabasalt sediments underlying the 100-N Area is described in terms of the sediments affecting the unconfined aquifer and vadose zone (Figure 6). These sediments have been subdivided into the Ringold Formation of Pliocene age and the Hanford formation (informal) of Pleistocene age.

3.1 RINGOLD FORMATION

Brown (1962), Tallman et al. (1979), Routson and Fecht (1979), and Bjornstad (1984, 1985) have divided the Ringold Formation into basal, lower, middle, and upper units based on sediment textures in the central part of the Hanford Site. All of these units are not present in the 100-N Area. Gilmore et al. (1990) have divided the Ringold Formation into three distinct units in the 100-N Area: an indurated sandy gravel, a muddy silt, and a sandy gravel.

The indurated sandy gravel unit unconformably overlies the basalt at approximately 23.8 m below mean sea level (msl) or 158.5 m below the land surface. This unit is 10.7 m thick and is overlain by the muddy silt that extends to approximately 30.5 m below the land surface. The top of this muddy silt forms the base of the unconfined aquifer. Overlying the muddy silt is a 12.2- to 18.3-m-thick sandy gravel unit in which the unconfined aquifer occurs. The contact between the Ringold Formation and the overlying glaciofluvial sediments is approximately 18.3 m below the land surface. The Ringold Formation is differentiated from the glaciofluvial sediments of the Hanford formation by fewer basalt-rich and more quartz- or silica-rich cobbles and pebbles.

3.2 HANFORD FORMATION

The glaciofluvial sediments overlying the Ringold Formation are glacial flood sediments. These sediments were deposited when ice-dammed lakes within the Columbia River drainage released catastrophic torrents of water and ice when the ice dams were breached during Pleistocene glaciation (Bretz 1959, Baker 1973, and Waitt 1980). These sediments in the Pasco Basin have been informally named the Hanford formation and have been divided into a coarse-grained sand and gravel known as the Pasco gravels (Brown 1975) and a fine-grained sand and silt termed the Touchet beds (Flint 1938). These deposits vary abruptly both vertically and laterally, reflecting the depositional environment. The Pasco gravels were deposited in high-energy areas of rapid flow; the Touchet beds were deposited in low-energy or slack-water environments. The Pasco gravels are prevalent in the 100-N Area. Near the 1301-N LWDF, from the top of the Ringold Formation to 4.6 m below the surface, the sediments are silty sandy gravel with scattered boulders. The upper 4.6 m of the sediments consist of 20% cobbles and boulders in a coarse-grained sandy matrix.

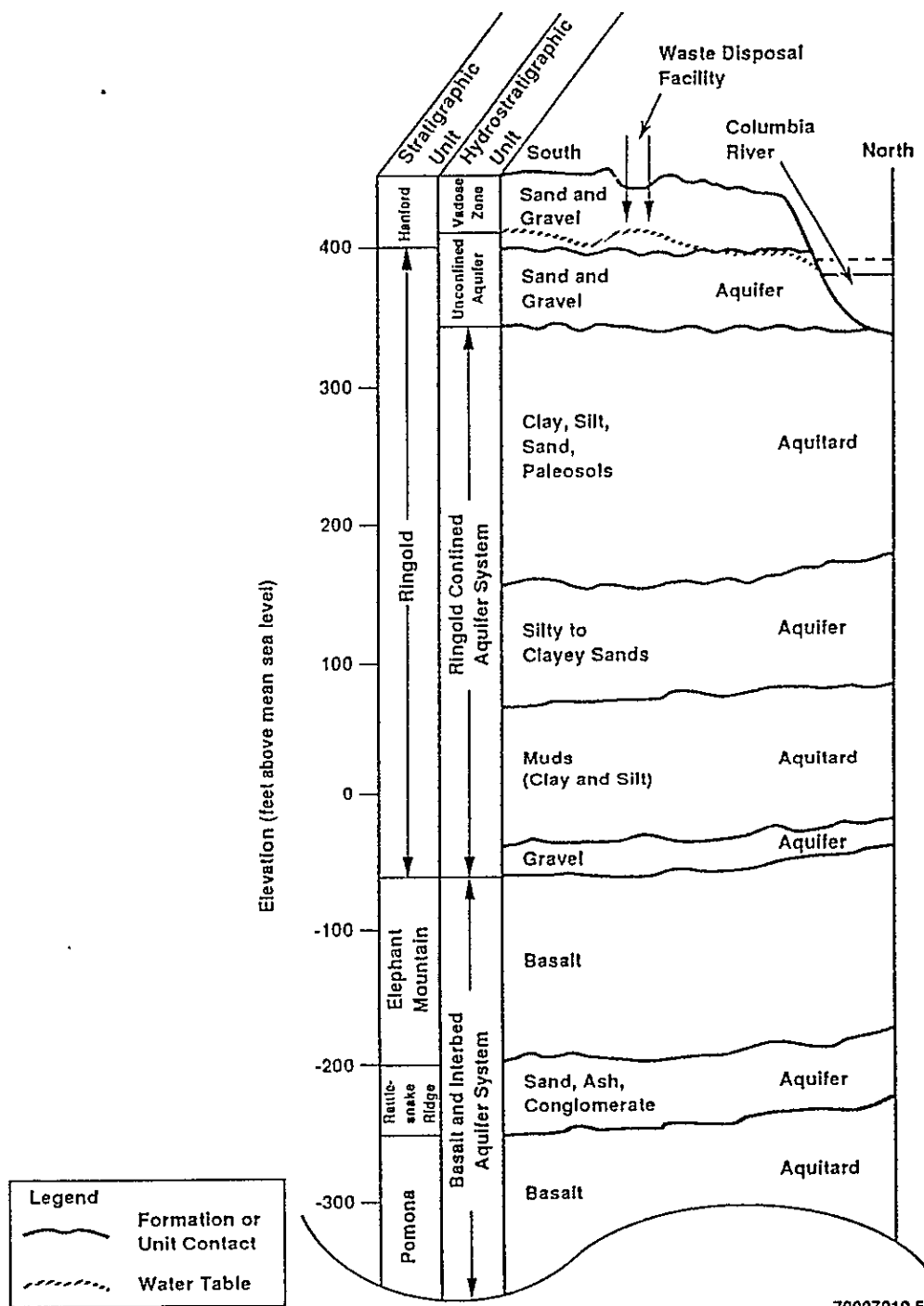


Figure 6. Near-Surface Hydrogeologic Units in the 100-N Area.

4.0 MODEL DESCRIPTION

In the plan view, the conceptual model (Figure 7) encompassed an area of approximately 1,880,000 m² oriented parallel to the Columbia River (N35°E).

4.1 GEOMETRY

The dimensions of the model were 1,615 m in a SW-NE direction and 1,164 m in a SE-NW direction. The model dimension in a vertical direction was approximately 28.5 m from the land surface to 9 to 11 m below the water table as it existed before the 100-N Area LWDFs became operational. The Columbia River bounds the northwest face of the model. The Hanford and Ringold Formations are modeled as distinct units.

The unconfined aquifer is located between the water table and the top of the muddy silt unit of the Ringold Formation. The water table in the western part of the Hanford Site is at the top of the Ringold Formation (Figure 8) (DOE 1987). Two relative positions of the water table are shown in Figure 8. The lower position is based on the average minimum flow rate of the Columbia River; the upper position is based on the average maximum flow rate.

Localized mounding of the water table occurred beneath the 100-N LWDFs. Where this mounding occurred, the lower portion of the Hanford formation remained saturated during the operation of the LWDFs. The thickness of the unconfined aquifer varies from 9.1 to 15.2 m. The unsaturated zone is composed primarily of the sediments of the Hanford formation. The unsaturated zone varies from zero adjacent to the Columbia River to approximately 18.3 m thick along the southern boundary of the conceptual model.

4.2 SOURCE TERMS

For the numerical model to accurately predict the movement of contaminants in the groundwater, an accounting of the mass introduced into the LWDFs during operations must be established. The time simulated began at the time the LWDFs became operational. The 1301-N and 1325-N Facilities consist of rectangular, covered, pond-like enclosures termed "cribs" which are designed to overflow into covered trenches that can accommodate large volumes of effluent discharge. Both of these LWDFs have been used to dispose of water contaminated with radionuclides. Hence, they are the source terms of the conceptual model for both contaminants and groundwater. Because no radionuclides were present in the water discharged to the 1324-N/NA LWDF, this facility is a source term only for groundwater recharge.

The 1301-N LWDF was the only facility used to dispose of effluent with radionuclides from late 1963 until late 1983. In 1965, when the waste water volume exceeded the capacity of the facility, an extension trench was added. The 1325-N LWDF was built to replace the 1301-N LWDF and became operational in 1983. However, shortly after the start of operations at 1325-N, it became

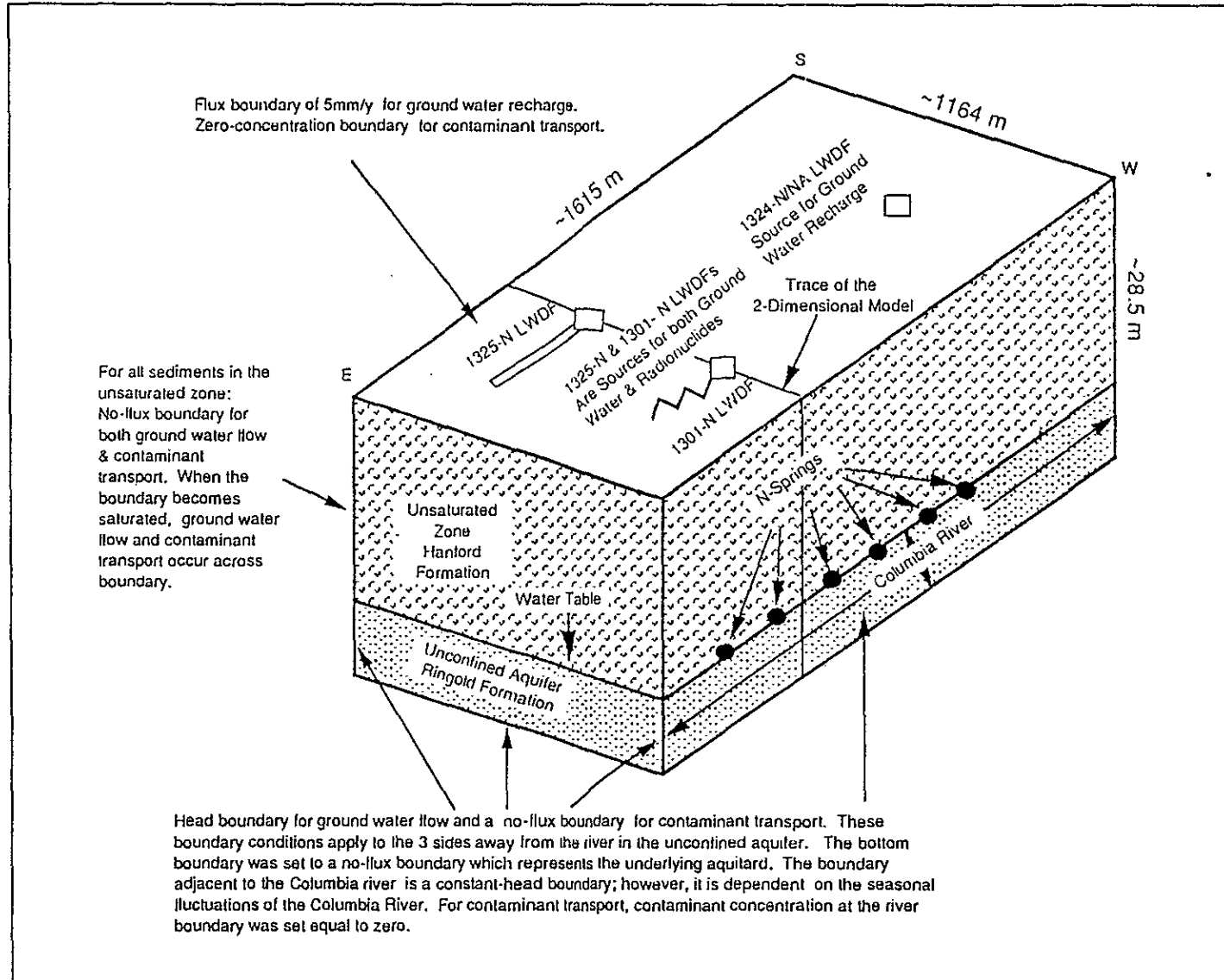


Figure 7. Conceptual Model for the Numerical Simulation for the 100-N Area N Springs Project.

9513381.0033

WHC-SD-ER-TA-001

Figure 8. Geologic Cross Section of the 100-N Area.

apparent that the 1325-N LWDF would not be able to accommodate the entire volume of effluent; hence, the remainder was discharged to the 1301-N Crib. The split in effluent discharge continued until September 19, 1985, at which time the 1325-N LWDF became fully operational. Except for very brief intermittent discharges to the 1301-N Facility, all radioactive effluent discharges since September 19, 1985 have been to the 1325-N Facility. The quantities of effluent discharged to each LWDF are given in Table 4 and Figure 9.

4.3 BOUNDARY CONDITIONS

The following boundary conditions were used for the flow equation of the numerical model. The regional groundwater system in 1964 had a hydraulic gradient of -0.00095 m/m (DOE 1987) from trending approximately south to north. A head boundary equal to the regional hydraulic gradient was imposed on the unconfined aquifer for the northeast, southwest, and southeast sides of the model (Figure 7). The flow-affecting condition for these boundaries, at the beginning of the simulation, was defined as the hydraulic heads before the start of LWDF operations. To derive the head boundary condition along one of these faces, the following equations can be used:

$$\text{Head}_{(\text{SE})} = 119.5 + ((-0.00095/2^{0.5}) * \text{distance along SE Boundary})$$

$$\text{Head}_{(\text{SW})} = 119.5 + ((-0.00095/2^{0.5}) * \text{distance along SW Boundary})$$

$$\begin{aligned} \text{Head}_{(\text{NE})} = 119.5 + ((-0.00095/2^{0.5}) * \text{Length of SE Boundary} \\ + \text{Distance along NE Boundary}) \end{aligned}$$

For the unsaturated zone, a no-flux boundary condition was imposed until the grid nodes next to the boundary became saturated. Once these nodes became saturated, the boundary was made permeable to the passage of groundwater by setting the boundary pressure equal to zero. This only occurred on the boundary next to the Columbia River.

The presence of the Columbia River was simulated by a constant-head boundary that was made equal to the seasonal elevation of the river (i.e., the boundary was made to change as a function of time). The bottom boundary of the model domain was defined in terms of a no-flow condition to represent the top of the aquitard (Figure 6). The flux at the upper boundary of the model domain was calculated from the initial moisture content.

For the contaminant transport equation, the top boundary was made equal to zero concentration. All of the other boundaries for the transport equation were defined as no-flux boundaries. This boundary condition applied to the dispersive and diffusive, but not to the advective part of the transport equation. Consequently, contaminants moved by advection were permitted to

Table 4. Source-Term Values Assigned for the Numerical Model.

| Year | Water flow to 1301-N LWDF (L/d) | Water flow to 1325-N LWDF (L/d) | Water flow to 1324-N LWDF (L/d) | Average ⁹⁰ Sr concentration in discharges (pCi/L) |
|-----------|---------------------------------------|---------------------------------------|---------------------------------------|---|
| 1964 | 9,462,500* | 0 | 0 | 20,000* |
| 1965 | 9,462,500* | 0 | 0 | 20,000* |
| 1966 | 9,462,500* | 0 | 0 | 20,000* |
| 1967 | 9,462,500* | 0 | 0 | 20,000* |
| 1968 | 9,462,500* | 0 | 0 | 20,000* |
| 1969 | 9,462,500* | 0 | 0 | 20,000* |
| 1970 | 9,462,500* | 0 | 0 | 20,000* |
| 1971 | 9,462,500* | 0 | 0 | 20,000* |
| 1972 | 9,462,000* | 0 | 0 | 20,000* |
| 1973 | 8,702,000 | 0 | 0 | 4,700 |
| 1974 | 9,500,000 | 0 | 0 | 18,100 |
| 1975 | 9,500,000 | 0 | 0 | 26,800 |
| 1976 | 9,900,000 | 0 | 0 | 30,400 |
| 1977 | 14,500,500 | 0 | 1,703,250 | 22,700 |
| 1978 | 12,500,000 | 0 | 1,703,250 | 26,300 |
| 1979 | 13,500,000 | 0 | 1,703,250 | 26,400 |
| 1980 | 12,500,000 | 0 | 1,703,250 | 35,000 |
| 1981 | 10,500,000 | 0 | 1,703,250 | 21,900 |
| 1982 | 10,500,000 | 0 | 1,703,250 | 36,500 |
| 1983 | 6,942,000 | 1,960,000 | 1,703,250 | 43,500 |
| 1984 | 8,100,000 | 1,900,000 | 1,703,250 | 84,800 |
| 1985 | 7,200,000 | 2,800,000 | 1,703,250 | 65,700 |
| 1986 | 0 | 7,250,000 | 1,703,250 | 13,600 |
| 1987 | 0 | 2,100,000 | 1,703,250 | 19,600 |
| 1988 | 0 | 1,660,000 | 1,703,250 | 24,700 |
| 1989 | 0 | 1,660,000 | 1,703,250 | 64,300 |
| 1990 | 0 | 1,660,000 | 1,703,250 | 64,300 |
| 1990-2020 | 0 | 0 | 0 | 0 |

*There is no reliable data available for average flow rates and average of the effluents discharged to the 1301-N crib. Rough estimates based on discharge volumes from 1973 to 1976 were used for 1964 through 1972. Data for 1973 through 1989 were taken from the yearly effluent-release reports.

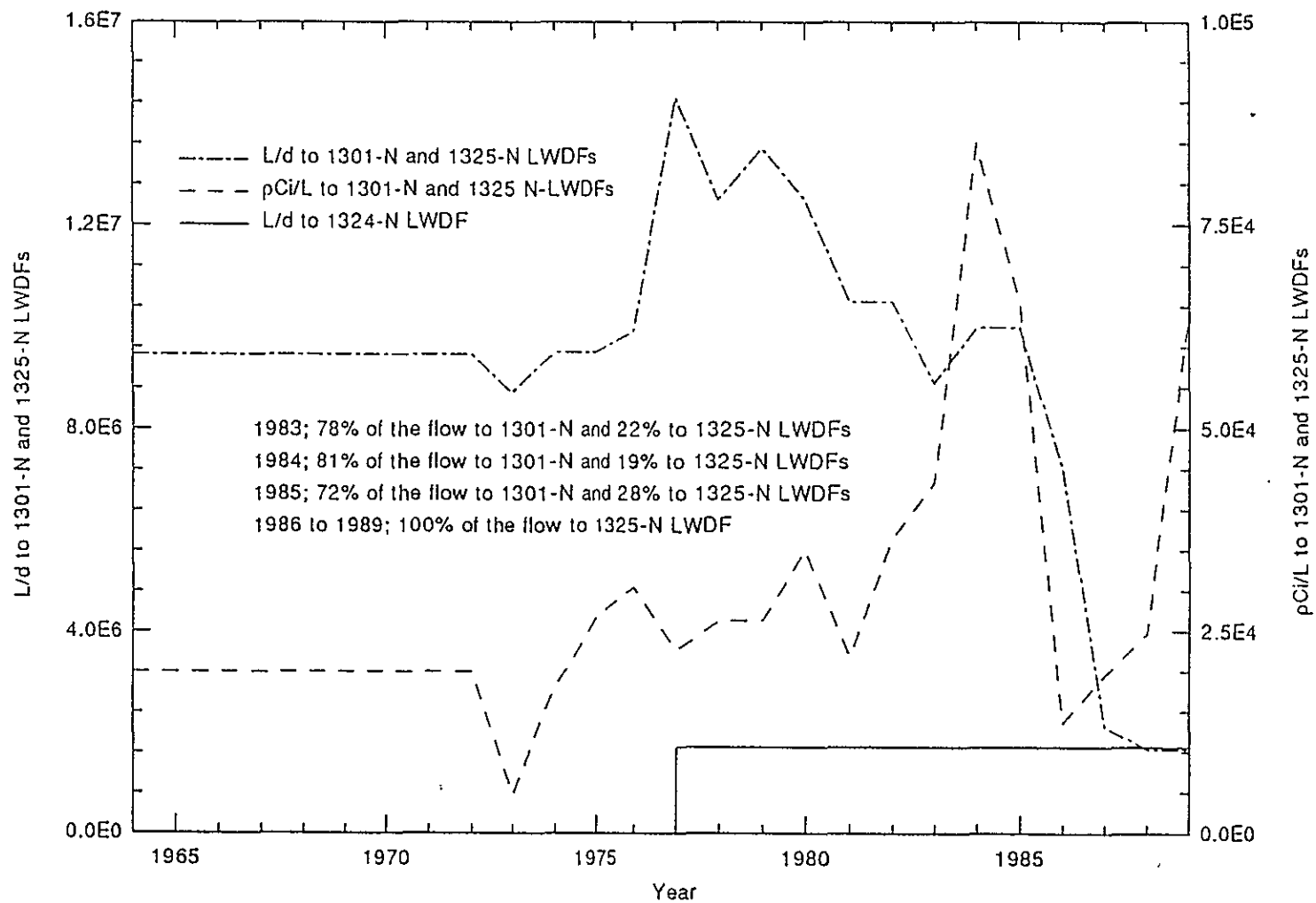


Figure 9. Average Effluent Flows and ^{90}Sr Concentrations Received by the 1301-N, 1324-N/NA, and 1325-N Liquid Waste Disposal Facilities.

leave the system at the boundaries of the model domain. Simulated groundwater moving through the boundaries was monitored by the PORFLO-3 software to account for the mass of contaminant leaving the system. A summary of each assigned boundary condition is provided in Table 5.

4.4 NUMERICAL DISCRETIZATION

The numerical simulations were performed using a three-dimensional cartesian grid. The axes of the system were aligned SW-NE (X-axis parallel to the Columbia River), SE-NW (Y-axis), and vertically (Z-axis) (Figure 10). The grid was converted into discrete data with 34,816 finite-difference cells (34 in the X-axis direction, 32 in the Y-axis direction, and 32 in the Z-axis direction). A variable grid spacing was used to accommodate the relatively large pressure gradients close to the sources and close to the Columbia River boundary. Near these features the grid is fine and away from these features the grid becomes coarse.

The physical features of the LWDFs that could not be incorporated into the numerical model were the extension trenches of the 1301-N and 1325-N LWDFs. The reason the trenches could not be incorporated was their narrow width relative to length. To convert these features into discrete data would have required excessive computer memory. To approximate the trenches in the numerical model, the surface areas at the bottom of the trenches were added to the surface areas of the crib bottom. Therefore, the source terms in the numerical model had the same surface areas as the cribs plus the trenches.

4.5 HYDROLOGIC PROPERTIES

In a deterministic model such as this, each material property can have only one value; this one value cannot represent the variability seen in the sediments present beneath the 100-N Area. Each hydrologic parameter used in the simulation and how their values were chosen are described in the following sections.

The values used are given in Table 6. For a two-dimensional simulation of groundwater movement and contaminant transport from the 100-N Area LWDFs, Lu (1990) used hydrologic parameters different from those used by this study. His values were a brief literature search made at the start of this study. Lu also did not have the results from the subsequently complete field sampling and testing. The values used here reflect the results of an extensive literature search and from the field sampling and testing in the 100-N Area that was a part of this study.

4.5.1 Soil Moisture Characteristics

No data were available to construct the moisture characteristic curves for the Hanford formation in the 100-N Area. Consequently, 10 undisturbed sites in the unsaturated zone that are down-gradient from the LWDFs were

Table 5. Assigned Boundary Types and Values.

| Boundary | Unsaturated Zone | | Unconfined Aquifer | |
|----------|---|---------------------------------|---------------------------------|---------------------------------|
| | Flow Equation | Concentration Equation | Flow Equation | Concentration Equation |
| Top | $\partial H / \partial Z = 0.005 \text{ m}$ | $C = 0.0$ | NA | NA |
| Bottom | NA | NA | $\partial H / \partial Z = 0.0$ | $\partial C / \partial Z = 0.0$ |
| NE | $\partial H / \partial X = 0.0$ | $\partial C / \partial X = 0.0$ | $H = 119.4 \text{ m}^a$ | $\partial C / \partial X = 0.0$ |
| SE | $\partial H / \partial Y = 0.0$ | $\partial C / \partial Y = 0.0$ | $H = 119.4 \text{ m}^a$ | $\partial C / \partial Y = 0.0$ |
| SW | $\partial H / \partial X = 0.0$ | $\partial C / \partial X = 0.0$ | $H = 119.4 \text{ m}^a$ | $\partial C / \partial X = 0.0$ |
| NW | $\partial H / \partial Y = 0.0^b$ | $\partial C / \partial Y = 0.0$ | $H = \text{SRL}^c$ | $C = 0.0$ |

^aThese boundaries provide an initial gradient of $\partial H / \partial L = -0.00965 \text{ m/m}$ from the south corner to the north corner of the model domain (Figure 10). See the equations in Section 4.3 to calculate the pressure at any position along these boundaries. The highest initial pressure within the model is 119.4 and it occurs at the southern corner of the domain.

^bThe boundary in the vadose zone is defined to be no-flow unless it becomes saturated; once saturated pressure head was set equal to 0. This allowed the flow of water across the boundary.

^cRefers to the seasonal variation of elevation of the Columbia River. Average high-flow elevation equals 118.5 m; average low-flow elevation equals 116.5 m; average median-flow elevation equals 116.5 m.

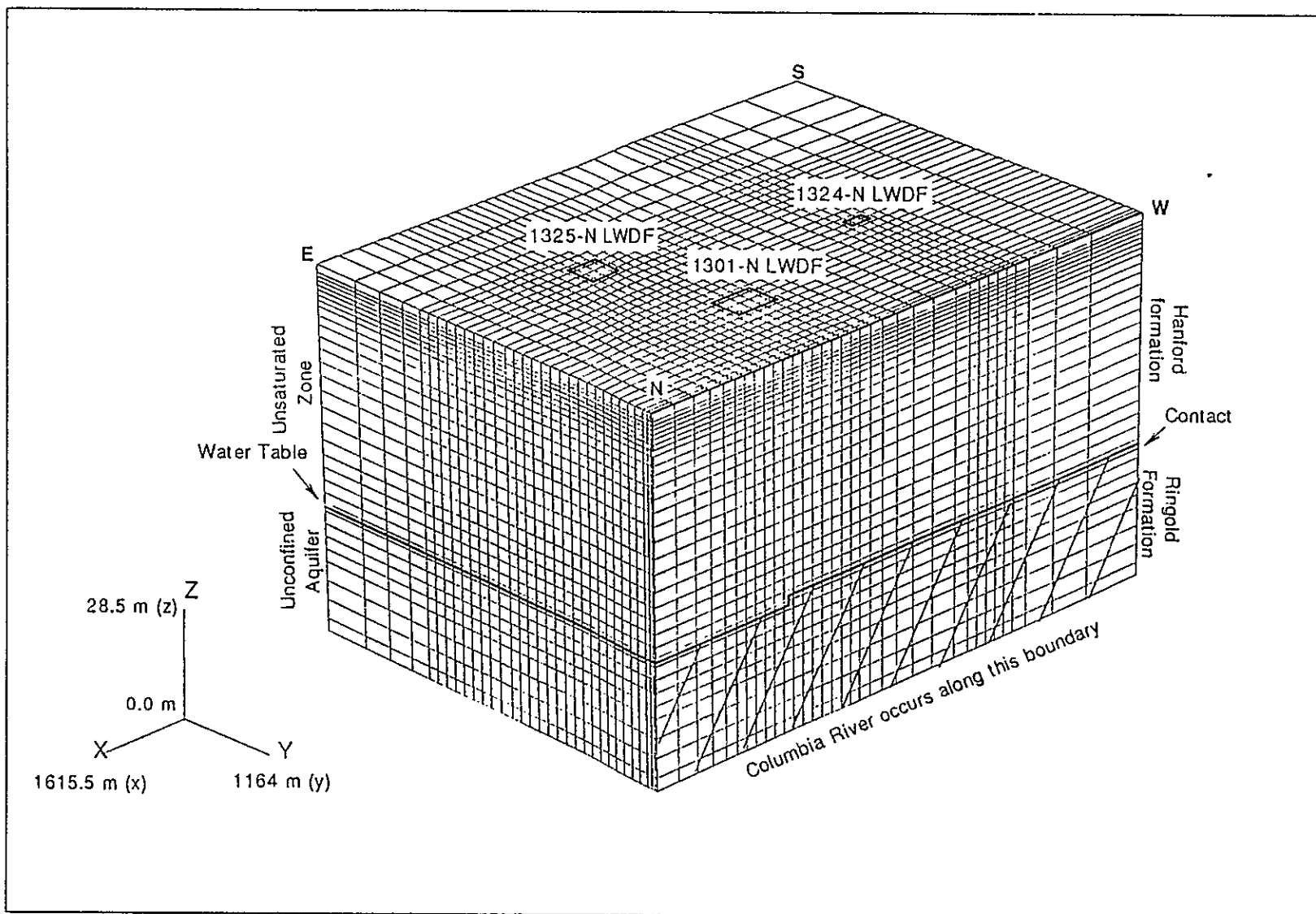


Figure 10. Numerical Grid Used in the 100-N Area Simulation.

Table 6. Hydrologic and Transport Properties Used in the Simulation.

| Flow parameters | Hanford formation | Ringold Formation | Crib floor |
|---|--|--|--|
| Saturated hydraulic conductivity | 3,600 m/yr (H) 360 m/yr (V) | 24,500 m/yr (H) 2,450 m/yr (V) | 3,600 m/yr (H) 360 m/yr (V) |
| Van Genuchten-Mualem soil moisture-characteristic parameters: Alpha N | 8.08/m 1.23 | N/A N/A | 8.08/m 1.23 |
| Effective porosity | 0.22 | 0.24 | 0.22 |
| Initial volumetric moisture content | 0.11 | N/A | 0.24 |
| Specific yield | N/A | 0.24 | N/A |
| | | | |
| Mass transport parameters | Hanford formation | Ringold Formation | Crib floor |
| Longitudinal dispersivity Alpha-L | 1.0 m | 1.0 m | 1.0 m |
| Transverse dispersivity Alpha-T | 0.1 m | 0.1 m | 0.1 m |
| Bulk density | 1.7 g/cm ³ | 1.6 g/cm ³ | 1.7 g/cm ³ |
| Molecular diffusivity | 4.42 x 10 ⁻⁴ m ² /yr | 4.42 x 10 ⁻⁴ m ² /yr | 4.42 x 10 ⁻⁴ m ² /yr |
| Sorption coefficient ⁹⁰ Sr | 30 m./g | 24.5 ml/g | 2200.0 ml/g |
| Half-life ⁹⁰ Sr | 28.6 yr | 28.6 yr | 28.6 yr |

H = Horizontal
V = Vertical

chosen for collection of samples for laboratory analyses. The results of the laboratory analyses were used to calculate Van Genuchten parameters for soil moisture characteristics (Van Genuchten 1985).

The results of the laboratory analyses and the results for the curves constructed from Van Genuchten's (1985) RETC program are shown in Figures 11 and 12, respectively. In analyzing the curves and discarding the outlying curves, the most representative curve was determined to be for Site 4 (Figure 13). This was the curve used in the simulation to represent the soil moisture characteristics of the Hanford formation. This moisture characteristic curve was important only in the early part of the simulation. Once the sediments underlying the LWDF became saturated, the saturated hydraulic conductivity was used. The hydrologic parameters derived from the data collected at all 10 field sites are shown in Table 7.

4.5.2 Saturated Hydraulic Conductivity

For the Hanford Site, published information indicates that the saturated hydraulic conductivity for the Hanford formation varies from 150 to 6,100 m/d; the saturated hydraulic conductivity for the middle unit of the Ringold Formation varies from 6 to 180 m/d (Gephardt et al. 1979). However, for this study, site-specific information on the saturated hydraulic conductivities specific to the 100-N Area was used for both the Hanford formation (unsaturated zone) and the Ringold Formation (unconfined aquifer). This site-specific information for the vadose zone is from the following sources: (1) saturated hydraulic conductivity measured as part of this study using Guelph Permeameters for sediments in the vadose zone at each of the 10 sites selected for measurement of soil moisture characteristics, (2) Brown and Rowe (1960), and (3) Pratt (1984).

Using the hydraulic conductivity values measured at the field sites and applying the formula from De Marsily (1986, p. 82) for averaging hydraulic conductivities, an average saturated hydraulic conductivity value of 4,090 m/yr was estimated. Brown and Rowe (1960) state that "experience at Hanford indicates that a conservative infiltration rate for this area is 10 to 20 g/d/ft² [149 to 298 m/yr]." This value is based on attainment of equilibrium after several months of facility operation and a head of 0.3 to 1.0 m of water.

In analyzing the performance of the 1325-N crib since the start of its operation in October 1983 to May 1984, Pratt (1985) noted that, although the design of the crib was based on an infiltration rate of 1,430 m/yr, by January 1984 the infiltration rate had dropped to 536 m/yr and by May 1984 it was down to 238 m/yr. In designing an extension trench to the 1325-N crib, Pratt (1985) conducted large-scale percolation tests on a test pond. The results from these tests indicated a minimum infiltration rate of 1,100 m/yr. However, this test lasted only 28 days and steady-state conditions may not have been obtained.

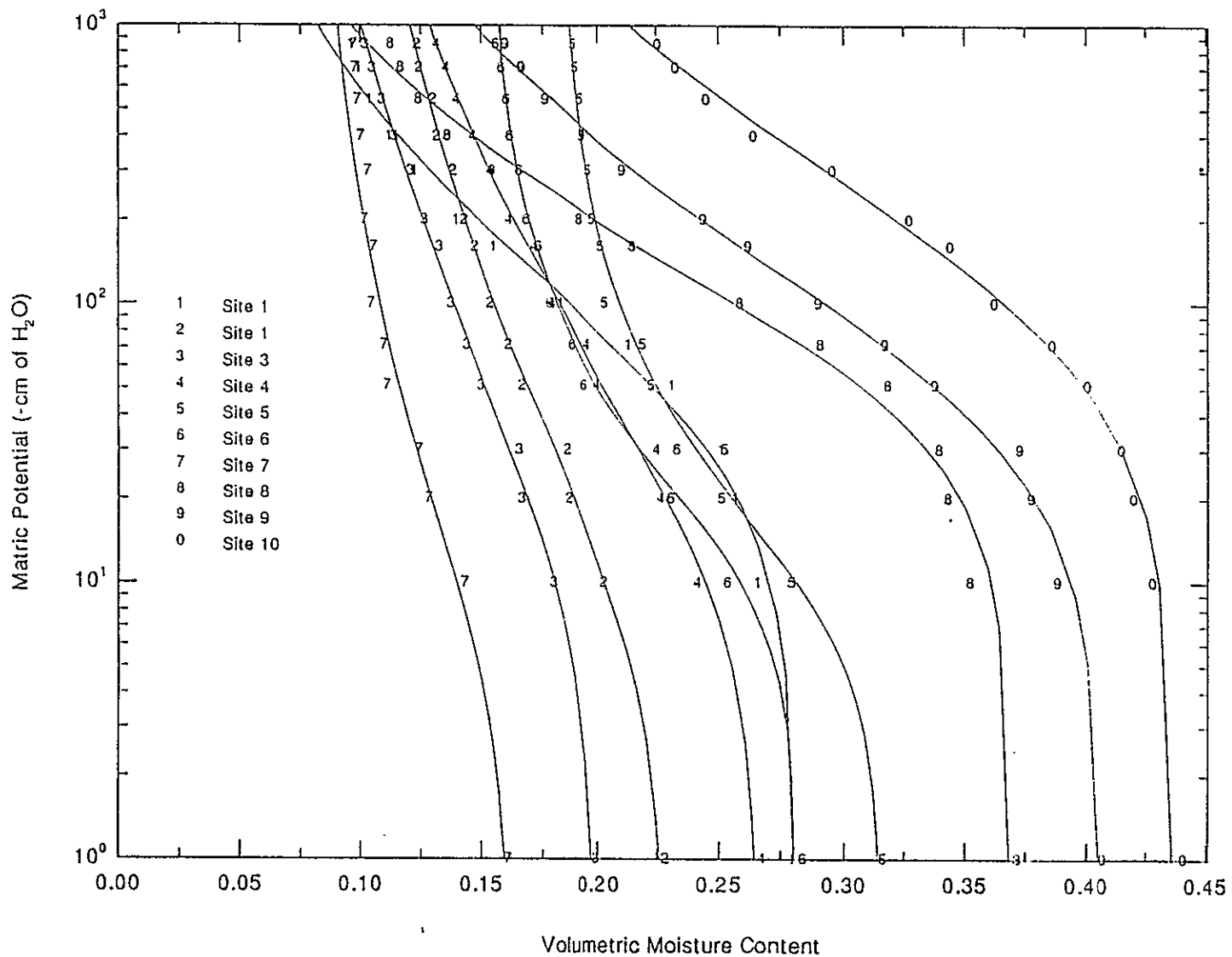


Figure 11. Comparison of Moisture Characteristic Data from the Field with Fitted Moisture Characteristic Curves using Van Genuchten (1985) RETC Program.

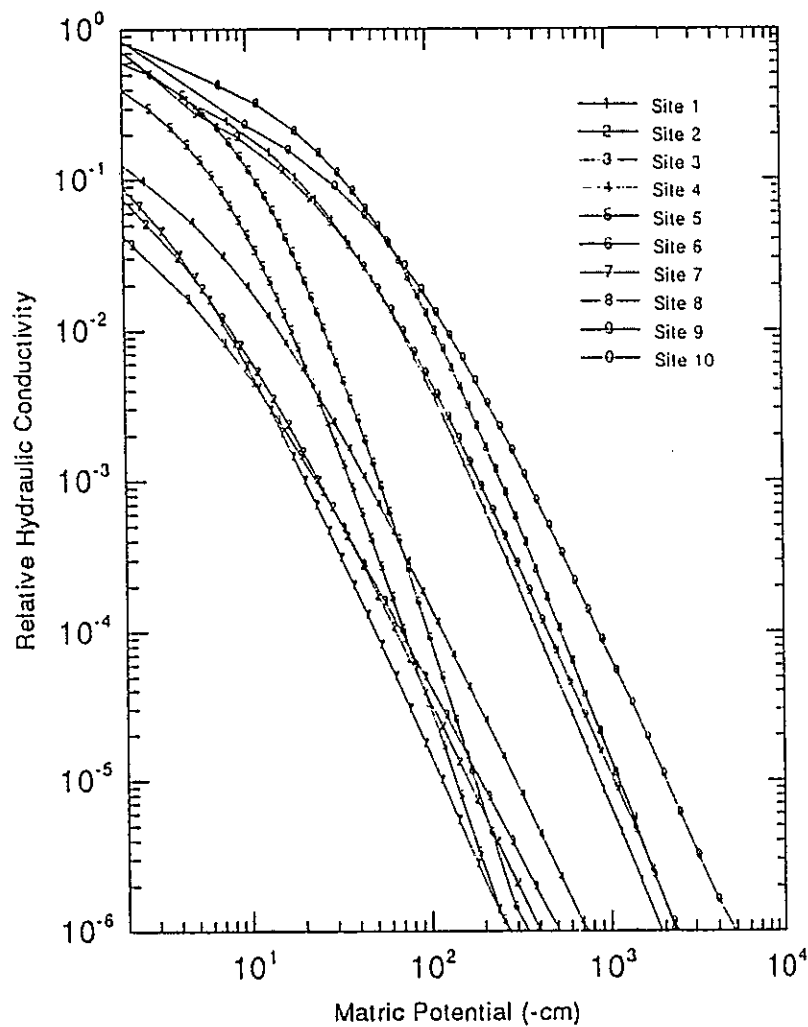


Figure 12. Relative Hydraulic Conductivities as a Function of Matrix Potential for the 10 Sites.

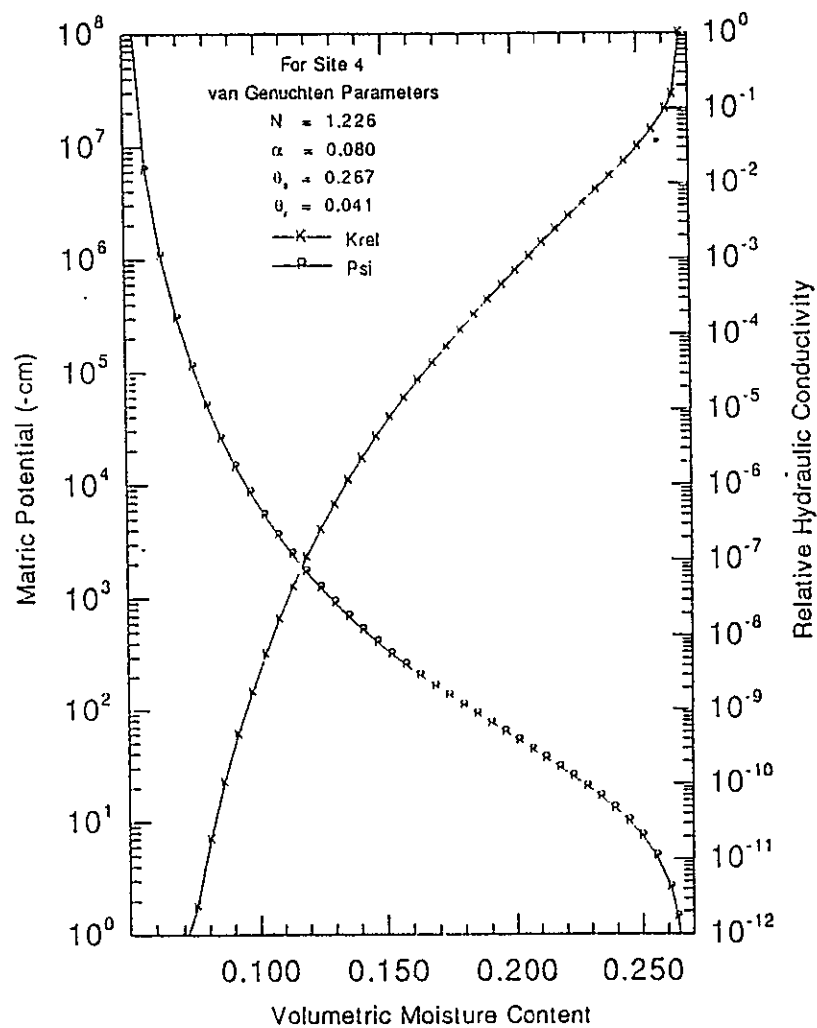


Figure 13. Moisture Characteristic Curves Showing Relative Hydraulic Conductivities and Matrix Potential as a Function of Volumetric Water Content.

Table 7. Hydrologic Parameters Derived from Field Sites
in the 100-N Area. (sheet 1 of 2)

| Parameter | Value | Parameter | Value |
|--------------------|------------|--------------------|------------|
| Site 1 | | Site 2 | |
| N | 1.390 E+00 | N | 1.223 E+00 |
| Alpha | 2.327 E-02 | Alpha | 1.461 E-01 |
| M | 2.805 E-01 | M | 1.826 E-01 |
| WCS | 2.806 E-01 | WCS | 2.286 E-01 |
| WCR | 0.000 E+00 | WCR | 6.801 E-02 |
| Effective porosity | 2.806 E-01 | Effective porosity | 1.606 E-01 |
| K(SAT) m/yr | 7.889 E+02 | K(SAT) m/yr | 9.783 E+03 |
| Site 3 | | Site 4 | |
| N | 1.143 E+00 | N | 1.226 E+00 |
| Alpha | 1.183 E-01 | Alpha | 8.008 E-02 |
| M | 1.250 E-01 | M | 1.842 E-01 |
| WCS | 1.989 E-01 | WCS | 2.667 E-01 |
| WCR | 0.000 E+00 | WCR | 4.703 E-02 |
| Effective porosity | 1.989 E-01 | Effective porosity | 2.196 E-01 |
| K(SAT) m/yr | 1.925 E+04 | K(SAT) m/yr | 7.258 E+03 |
| Site 5 | | Site 6 | |
| N | 1.629 E+00 | N | 1.759 E+00 |
| Alpha | 1.069 E-01 | Alpha | 7.016 E-02 |
| M | 3.861 E-01 | M | 4.315 E-01 |
| WCS | 3.155 E-01 | WCS | 2.810 E-01 |
| WCR | 1.794 E-01 | WCR | 1.524 E-01 |
| Effective porosity | 1.362 E-01 | Effective porosity | 1.286 E-01 |
| K(SAT) m/yr | 1.483 E+03 | K(SAT) m/yr | 1.010 E+04 |
| Site 7 | | Site 8 | |
| N | 1.312 E+00 | N | 1.482 E+00 |
| Alpha | 1.933 E-01 | Alpha | 1.616 E-02 |
| M | 2.380 E-01 | M | 3.254 E-01 |
| WCS | 1.619 E-01 | WCS | 3.689 E-01 |
| WCR | 7.352 E-02 | WCR | 0.000 E+00 |
| Effective porosity | 8.835 E-02 | Effective porosity | 3.689 E-01 |
| K(SAT) m/yr | 7.574 E+03 | K(SAT) m/yr | 1.578 E+02 |

Table 7. Hydrologic Parameters Derived from Field Sites
in the 100-N Area. (sheet 2 of 2)

| Parameter | Value | Parameter | Value |
|--------------------|------------|--------------------|------------|
| Site 9 | | Site 10 | |
| N | 1.333 E+00 | N | 1.294 E+00 |
| Alpha | 2.092 E-02 | Alpha | 1.107 E-02 |
| M | 2.495 E-01 | M | 2.269 E-01 |
| WCS | 4.058 E-01 | WCS | 4.365 E-01 |
| WCR | 0.000 E+00 | WCR | 0.000 E+00 |
| Effective porosity | 4.058 E-01 | Effective porosity | 4.365 E-01 |
| K(SAT) m/yr | 3.156 E+03 | K(SAT) m/yr | 1.262 E+03 |

WCS = Saturated volumetric water content

WCR = Residual volumetric water content

N = Van Genuchten curve-fitting parameter

M = Van Genuchten curve-fitting parameter

Alpha = Van Genuchten curve-fitting parameter

K(SAT) = Saturated hydraulic conductivity.

The maximum infiltration rate for saturated, steady-state conditions is equal to saturated hydraulic conductivity (Skaggs and Khaleel 1982). The range of observed infiltration rates for the unsaturated zone is from 240 m/yr at the 1325-N LWDF to 19,250 m/yr measured with a Guelph Permeameter at Site 3 (Figure 5). An explanation for the difference between the values measured at the LWDF and percolation test site and those measured by the Guelph permeameters could be that saturated hydraulic conductivity changed with time. This change could be because of realignment of fine soil and precipitate particles and a decrease of porosity in the sediments underlying the LWDF and percolation pond until an equilibrium value is attained. These factors would not be present at the Guelph Permeameter sites.

For the conceptual model used in this study, a saturated hydraulic conductivity of 360 m/yr was used for vertical flow in the unsaturated zone. This value is important because the vertical conductivity controls how rapidly the contaminants may potentially move downward through the unsaturated zone. The value used is believed to be conservative [i.e., 20% larger than the value reported by Brown and Rowe (1960) and 50% larger than the May 1984 infiltration rate from the 1325-N crib test]. This hydraulic conductivity is considerably smaller than that indicated by pump tests of both the Hanford formation and the upper Ringold Formation. Because pump tests measure horizontal conductivity and infiltration rates measure vertical conductivity, an anisotropy ratio of 1/10 vertical to horizontal conductivity was used throughout the model. This ratio compares favorably to the average saturated hydraulic conductivity values measured by the Guelph Permeameter.

The transmissivity of the Ringold Formation was measured from pump tests at wells N-34, N-32, and N-27 (Prater 1984). The transmissivity from these pump tests ranged from 539 to 2,415 m²/d. Using the thickness of the unconfined aquifer in those wells at the time of the pump tests yields hydraulic conductivities ranging from 39.3 to 176 m/d. The geometric mean of these hydraulic conductivities is 94 m/d. Brown (1964) reports a hydraulic conductivity value of 82 m/d. He also states that this value is somewhat high compared to sediments typical of the 100 Areas. Consequently, during the calibration phase of the work, this value was lowered to 67 m/d (Section 5.0).

4.5.3 Effective Porosity and Volumetric Moisture Content

The effective porosity used in modeling the vadose zone was 0.22. This number was calculated using Van Genuchten's (1985) RETC program and the moisture characteristic curve from field Site 4. The average volumetric moisture content from the 10 field sites was 0.13. Using this value and the unit gradient model, a natural recharge of 0.005 m/yr was calculated from the moisture characteristic curve. The effects of the natural recharge and the initial moisture content are insignificant when compared to the large volumes of water flushing through the LWDFs. For the unconfined aquifer, effective porosity varies from 0.05 to 0.3 (DOE 1987). An specific yield of 0.24 was used to represent the unconfined aquifer.

4.6 TRANSPORT PROPERTIES

The half-life of ^{90}Sr is 28.6 yr. No data exist for longitudinal and transverse dispersivities. These parameters are extremely difficult to measure. Typically, an assumption for longitudinal and transverse dispersivities is made. For this study, longitudinal and transverse dispersivities were assigned values of 1.0 m and 0.1 m. The bulk densities of the Hanford and Ringold Formations are 1.7 g/cc and 1.6 g/cc, respectively. Hajek (1968) reports that the molecular diffusion coefficient for the Hanford and Ringold Formations is $4.42 \times 10^{-4} \text{ m}^2/\text{yr}$ and the retardation coefficient (R_d) is 100 for ^{90}Sr . The corresponding distribution coefficient (K_d) for this R_d for the Hanford formation is 30 mL/g and for the Ringold Formation it is 24.5 mL/g.

9513381.0048

WHC-SD-ER-TA-001

This page intentionally left blank.

5.0 MODEL CALIBRATION

The unsaturated zone and unconfined aquifer comprise the sediments that are extremely heterogenous. Measurements of saturated hydraulic conductivity, volumetric soil moisture content; Van Genuchten soil moisture curve-fitting parameters; and sorption coefficients, boundary conditions, and source terms can vary by up to several orders of magnitude. Therefore, the first task was to calibrate the numerical model to observed field data. The hydraulic conductivity and the sorption coefficient were the only parameters adjusted for the calibration. This calibration to field data was an approximation only; it does not imply that the values used in the simulation are the actual hydrologic and contaminant transport properties of the 100-N Area; rather, the calibration highlights indicate where additional data should be collected.

5.1 CALIBRATION OF THE GROUNDWATER FLOW EQUATION

The first task was to calibrate the groundwater flow of the model. This was done by comparing simulated arrival times of a nonsorbed radionuclide and water table elevations in July 1969 to observed field data. Crews and Tillson (1969) correlated concentration peaks for ^{131}I from the time the effluent was introduced into the 1301-N LWDF following a fuel element failure at N Reactor, to the appearance of a corresponding concentration peak in down-gradient wells and riverbank springs. From the associated peaks, they calculated the travel time to be from 9 to 17 days for ^{131}I . However, this travel time is dependent on the elevation of the river.

At lower river elevations, the pressure gradient would be larger, causing the travel time to decrease. At higher river elevations, the gradient would be smaller, causing the travel time to increase. Figure 14, based on the shortest flow path, shows the effect of a rise in river elevation at 0.125 yr from the start of the simulation; the concentration of ^{131}I decreases until equilibrium is again achieved, at which time clean water from the river moves into the aquifer. After the river comes to equilibrium with the discharge from the crib, the concentration again begins to rise.

Using the hydraulic conductivity given in Table 6 for the unconfined aquifer, the PORFLO-3 software calculated a travel time of 43 d (Figure 14). This time is approximately 3.5 times longer than that determined by Crews and Tillson. The PORFLO-3 simulation could be made to match the results of Crews and Tillson provided that the hydraulic conductivity of the unconfined aquifer was increased. However, when using a hydraulic conductivity of the unconfined aquifer calibrated to the travel time calculations, the PORFLO-3 results underpredicted the elevation of the water table (Figures 15 and 16).

To correctly predict the elevation of the water table, the PORFLO-3 software required a hydraulic conductivity for the unconfined aquifer that was lower than that in Table 6. The discrepancy between the travel time measurements and the water table elevation is most likely due to lenses of clay and silt with low hydraulic conductivities interspersed with the gravels and sands that compose most of the unconfined aquifer and vadose zone (Figure 8). Consequently, the hydraulic conductivity used in the model

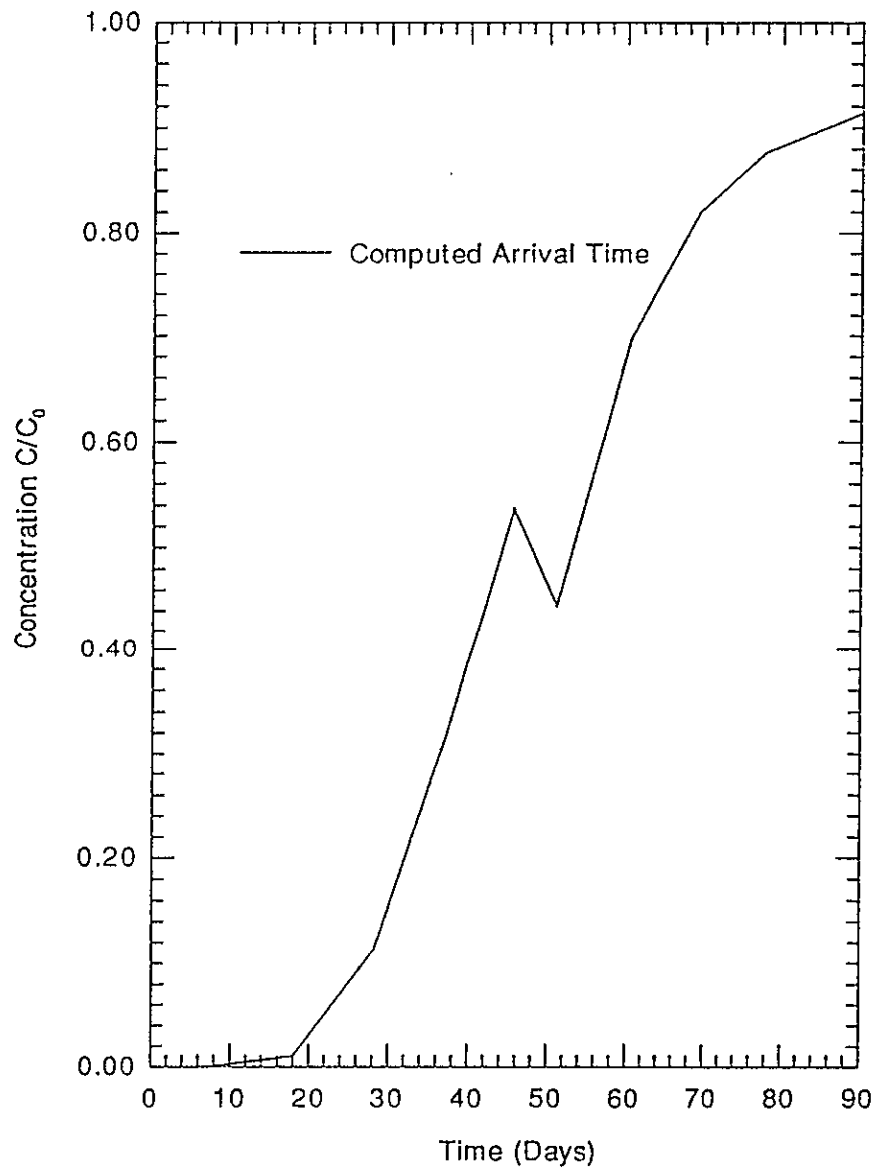


Figure 14. Calculated Arrival Time of a Nonsorbed Solute. The decrease in concentration at 1.25 yr is due to a higher elevation of the Columbia River.

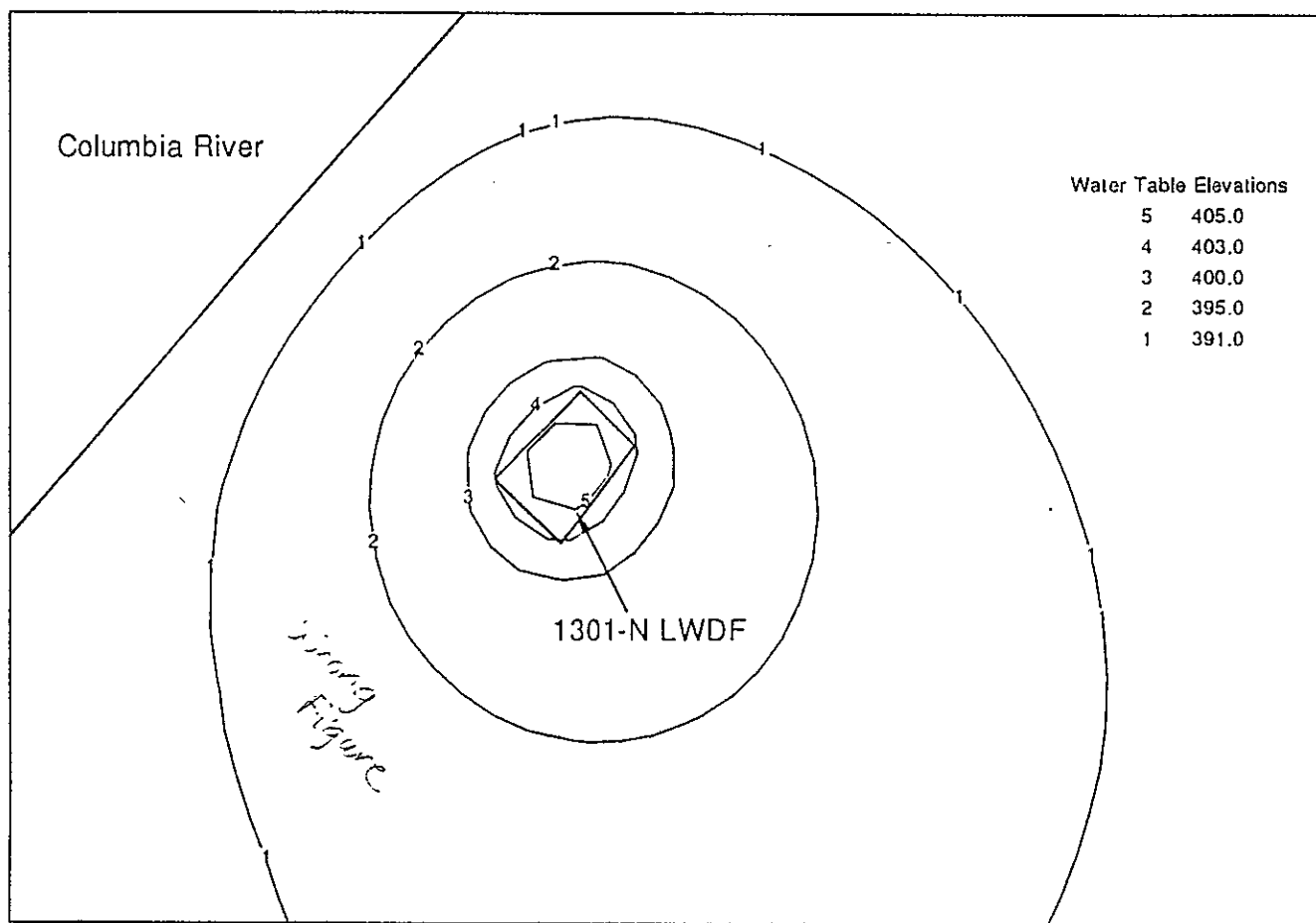


Figure 15. Observed Water Table Elevations in July 1969.

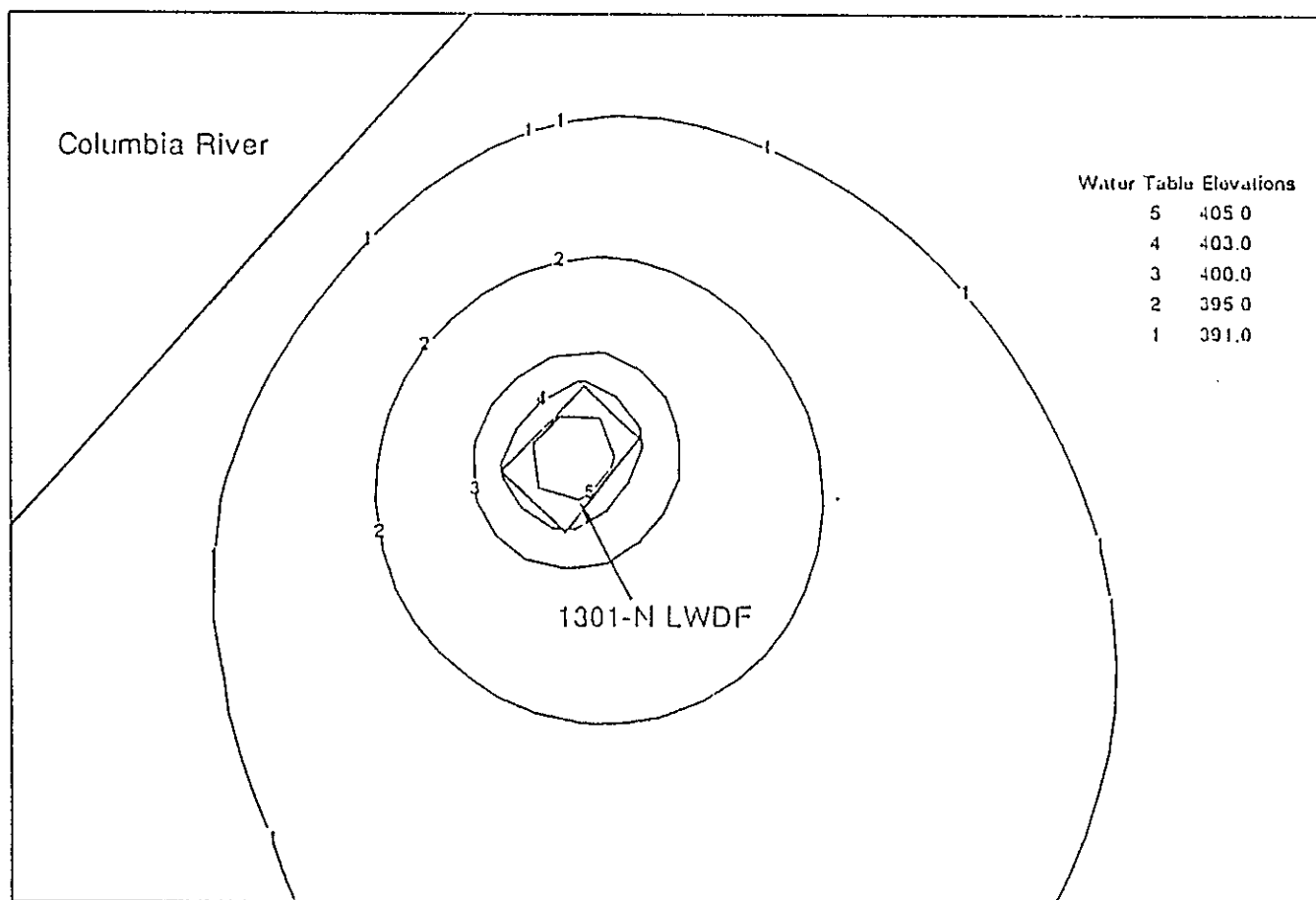


Figure 16. Water Table Elevations Simulated by PORFLO for July 1969.

depicts a value between those derived from the travel time calculations and the observed water table elevation.

5.2 CALIBRATION OF THE CONTAMINANT TRANSPORT EQUATION FOR ^{90}Sr

The next task was to calibrate the arrival time of ^{90}Sr at the Columbia River to observed field data. The object of this part of the calibration was to match the concentration of ^{90}Sr to that in the samples collected at N Springs. This proved to be the most difficult part of the calibration because no data existed for the years 1964 to 1972. The amount of water and contaminant concentration being discharged to the 1301-N LWDF during those years was assumed to be similar to that recorded for 1973 through 1975. The PORFLO-3 software was run to simulate the years between 1964 and 1974. At the end of 1974, the concentration predicted by the model were approximately the same as those observed at N Springs.

The average measured concentration of ^{90}Sr at N Springs is only a small fraction of what was discharged to the 1301-N LWDF from 1973 to 1985 (Figures 17 and 18). Using a model without a zone of high sorption underlying the 1301-N LWDF, neither this study nor that of Lu (1990) was able to match the model results to the concentrations of ^{90}Sr observed at N Springs (e.g., Cucchiara 1975 through 1978, Greager 1979 through 1981, Fogel 1983, and Rokkan 1984 and 1985). Lu (1990) speculated that retardation mechanisms other than sorption were present. He suggested that the sludge layer at the bottom of the LWDFs consisting of calcium carbonate, iron oxide, and clay (Pratt 1984) acted as a filter for particulate ^{90}Sr . To model this layer, he assigned an unreasonably high sorption coefficient ($K_d=1628 \text{ mL/g}$) to address both filtering and sorption.

The same was done in this study except that a corresponding distribution coefficient of $2,200 \text{ mL/g}$ was assigned at the bottom of the LWDFs. This coefficient was higher than that used by Lu (1990). The use of different sorption coefficients by the two studies is related to the differences in thickness assigned to the layer. Lu (1990) used a thickness of 1.5 m ; this study used a thickness of 0.68 m . Because of the nonlinearity of hydraulic properties in the vadose zone, this study ended the calibration in 1974 when it appeared that the model was predicting the values actually observed at N Springs (Figure 18). In actuality, the PORFLO-3 simulation estimated an arrival time of ^{90}Sr that was 4 yr less than that observed and, hence, overpredicted the concentration of ^{90}Sr at N Springs. Consequently, although the model was not calibrated in an exact sense, it did approximate the groundwater flow and contaminant transport in the 100-N Area based on field observations.

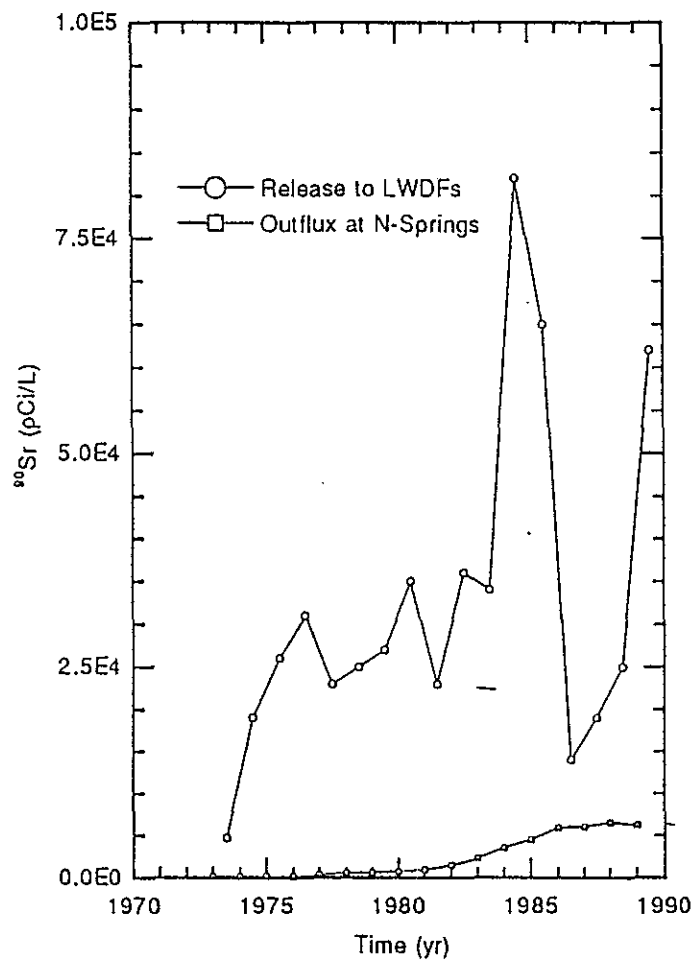


Figure 17. Observed Concentrations of ^{90}Sr at the 1301-N LWDF and N Springs.

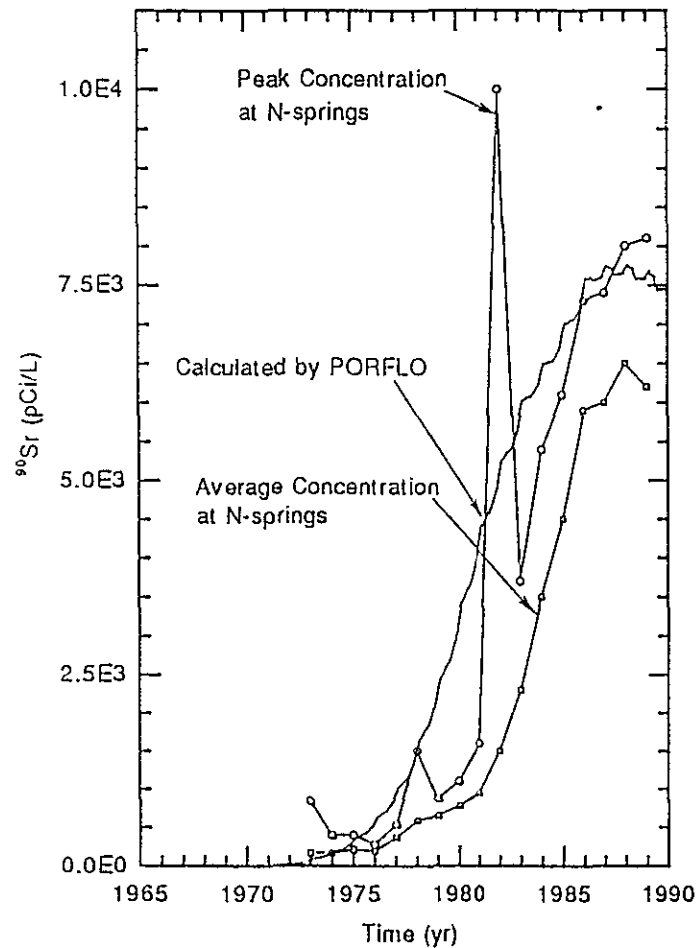


Figure 18. Observed and Simulated Peak Concentrations of ^{90}Sr at N Springs.

6.0 RESULTS OF THE GROUNDWATER FLOW AND CONTAMINANT TRANSPORT ANALYSES

The effects of the following variables on groundwater flow and contaminant transport were simulated: seasonal river-level fluctuations, average annual discharge of effluents to the three LWDFs in the 100-N Area, and the annualized average concentration of ^{90}Sr discharged to the 1301-N and 1325-N LWDFs. The results of the simulations are summarized in five figures. Streamlines indicating the direction of groundwater flow at the time noted are shown on each figure. Two planes through the conceptual model are shown. One is a planar view (i.e., X-Y plane) at a Z-axis depth of 20.5 m below ground surface. The other is a cross-sectional view (i.e., Y-Z plane) through the 1301-N LWDF at an X-axis distance of 1082.4 m from the origin of the conceptual model axes (Figure 10). The two views can be distinguished from one another by their axis labels.

6.1 GROUNDWATER FLOW

Before discharges to the LWDFs in the 100-N Area, the hydraulic gradient of the 100-N Area was -0.000965 in a northerly direction (DOE 1987). This hydraulic gradient was used to extrapolate the initial conditions (Figure 19a) in the unconfined aquifer at the start of LWDF operations in late 1963. Shortly after the start of operations, a wetting front began to form (Figure 19b). The wetting front continued to move downward until it intersected the water table 1.5 mo after the start of LWDF operations (Figure 19c), forming a conduit for effluent flow from the LWDF to the unconfined aquifer. As more effluent was discharged to the 1301-N LWDF, the water table began to rise beneath the LWDF (Figures 19c through 20b), forming a well-defined mound. By 1969, nearly steady-state conditions had occurred (Figure 20c), with the discharge to the LWDF dominating the flow regime. The seasonal river-level changes are shown to have little influence on the size of the water-table mound. This can be seen by comparing contour 6 for 1969 on Figures 20c (low-river level), 20d (medium-river level), and 20e (high-river level). In each figure, contour 6 remains approximately the same. However, the different river elevations do change the hydraulic gradient between the LWDF and the Columbia River. These steady-state groundwater conditions in the 100-N Area prevailed through 1976 (Figure 20f).

In 1977, the 1324-N/NA facility began to receive liquid effluent, causing a small rise in the water table beneath the facility. The flow system again rapidly reached a steady-state condition, with contour 6 moving towards the upper-left corner of Figure 21a. The flow from the 1301-N LWDF remained dominant, with effluent discharge to the 1324-N/NA LWDF being diverted to the west by the flow from the 1301-N LWDF. In 1983, approximately 20% of the flow to the 1301-N LWDF was diverted to the 1325-N LWDF. This diversion resulted in reducing the water-table mound beneath the 1301-N LWDF, developing a water-table mound beneath the 1325-N LWDF, and reducing diversion to the west of effluent from the 1324-N/NA LWDF. In late September 1985, the 1325-N LWDF became fully operational and, except for small intermittent discharges to it, all liquid effluent discharges to the 1301-N LWDF ceased. The last year that the 1325-N LWDF received large volumes of liquid effluent was 1986 (Figure 9).

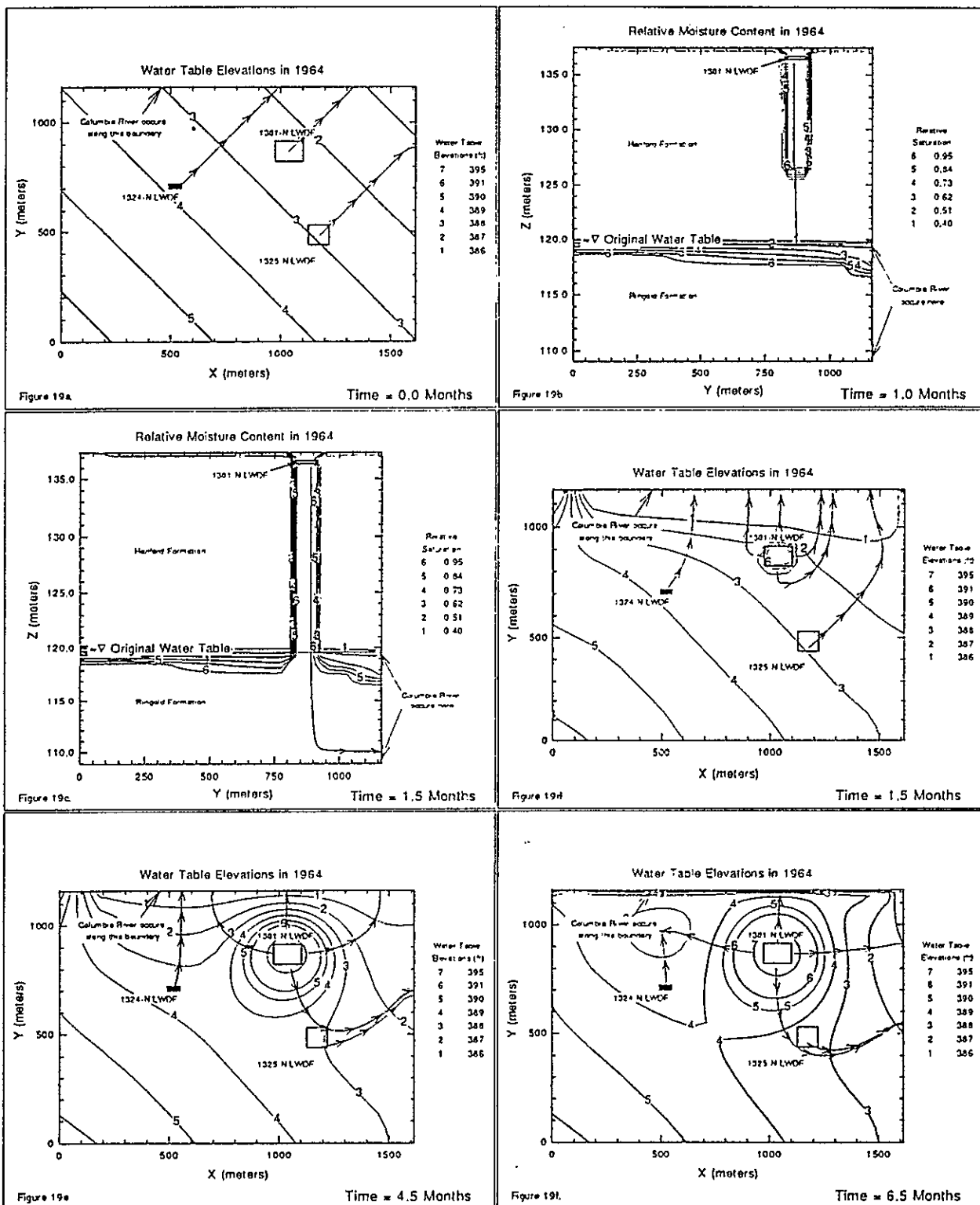


Figure 19. Selected PORFLO-3 Results Showing the Initial Conditions and the Rise in the Water Table Beneath the 1301-N Liquid Waste Disposal Facility.

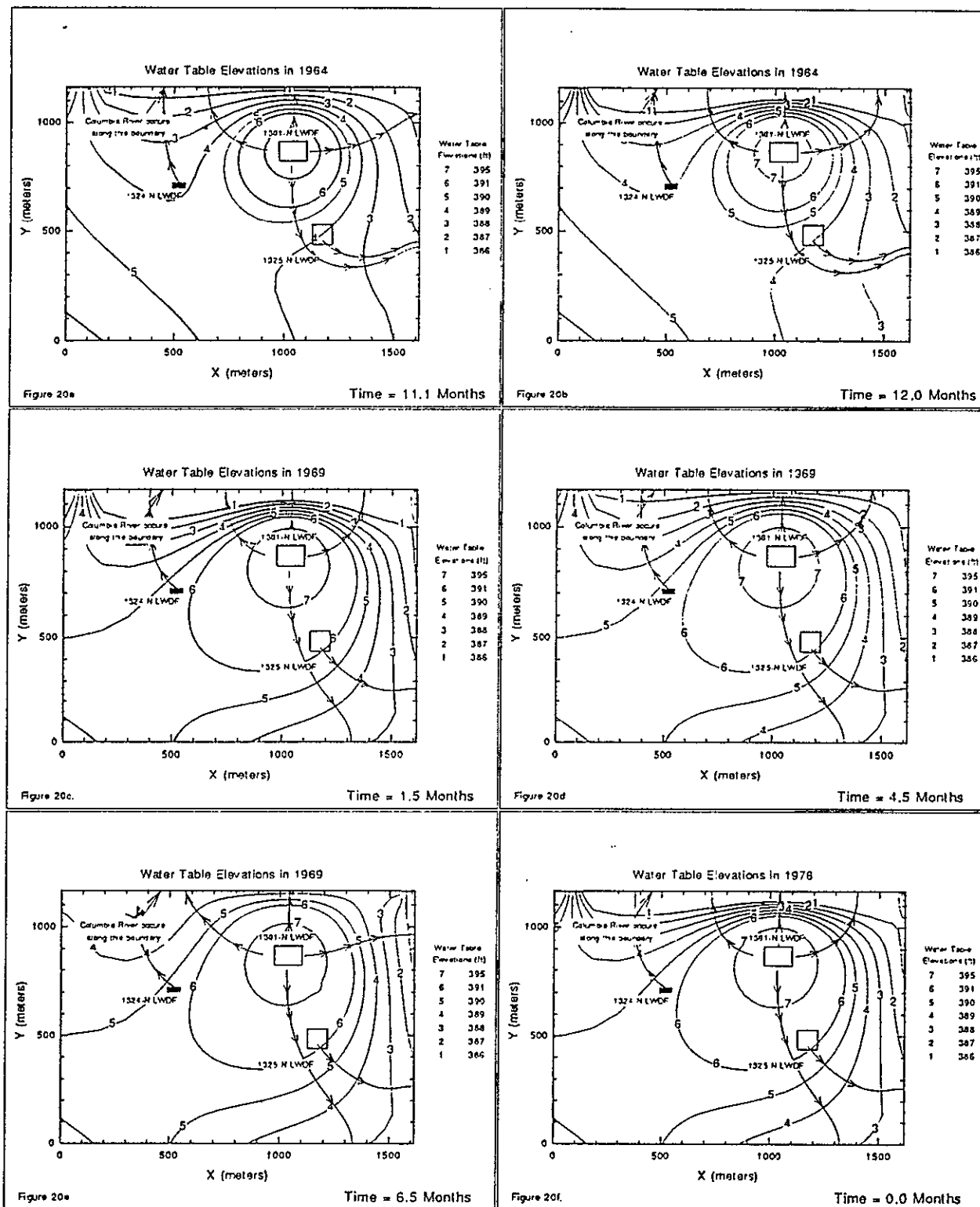


Figure 20. Selected PORFLO-3 Results Showing the Development of Steady-State Groundwater Flow Conditions Beneath the 1301-N Liquid Waste Disposal Facility.

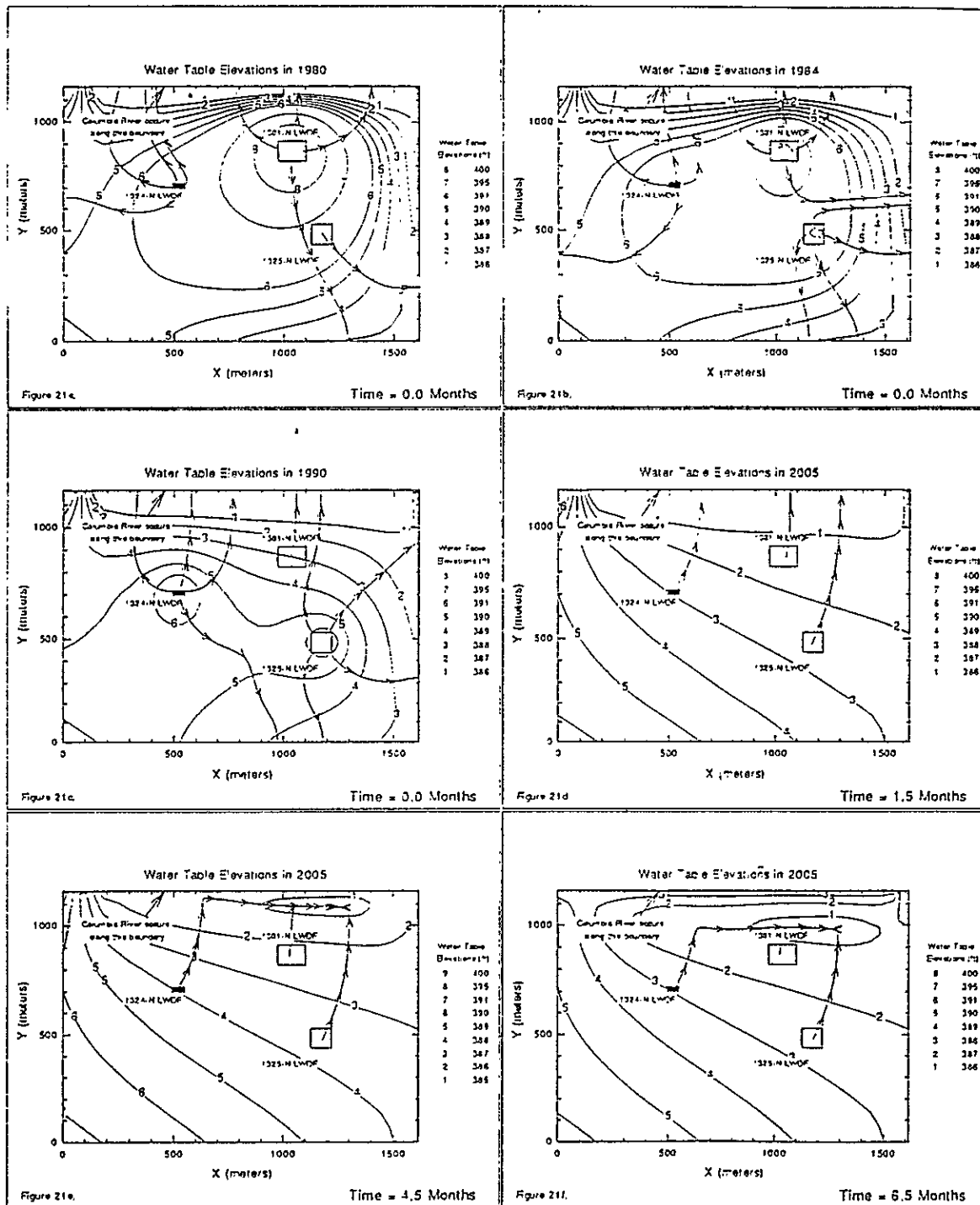


Figure 21. Selected PORFLO-3 Results Showing the Perturbation of Steady-State Conditions Caused by Effluent Discharges to the 1324-N/NA and 1325-N Liquid Waste Disposal Facility (21a through 21c) and the Interaction of the Columbia River with the Unconfined Aquifer (21d through 21f).

In January 1987, the status of the N Reactor changed from operational to cold standby. The discharge of liquid effluent to the 1325-N LWDF has gradually decreased and is expected to end by late 1990. This change in operational status of the N Reactor is reflected by the difference between contours 5 and 6 in Figures 21b and 21c; the change in operational status caused the water-table mound underlying the 100-N Area to shrink.

By late 1990, all liquid effluent discharges to the LWDFs in the 100-N Area ceased. Simulations for another 30 yr were then run to estimate the amount of ^{90}Sr that will reach the Columbia River during this time. The principle driving force for groundwater flow in the absence of effluent discharge is the original hydraulic gradient and the seasonal fluctuations of the Columbia River. The natural hydraulic gradient will cause water in the unconfined aquifer beneath a LWDF to move towards the northeast (Figure 19a). The interaction between the Columbia River and the aquifer will cause the same water to move towards the river (Figure 21d). However, the simulation did not account for the gradient in Columbia River elevation from SW to NE (-0.000256); rather, a constant-head boundary equal to the seasonal elevation of the river was assigned to the entire length of the conceptual model boundary. This omission would cause water starting at one of the LWDFs to move more directly towards the river than might otherwise occur.

Figures 21d through 21f show the path of water at river stages that vary from low to medium to high. At a low-river stage, the water travels towards the river. As the river rises to medium and high stages, the hydraulic gradient reverses and water flows from the Columbia River into the unconfined aquifer. This reversal of gradient would force the water to flow parallel to the river until the river level dropped, causing the water once again to move towards the river. This interaction between the river and the unconfined aquifer would cause a contaminant plume to follow a zigzag path to the river. The simulation used the hydraulic gradient reported at the start of LWDF operations in 1964. That gradient may have changed during the past 26 yr. The determination of the steady-state hydraulic gradient, once effluent flows to the LWDFs have ceased, is critical for estimating releases of ^{90}Sr to the environment.

6.2 CONTAMINANT TRANSPORT

From both the 1301-N and 1325-N LWDFs, the ^{90}Sr plume moves vertically downward through the vadose zone with little lateral movement. This is shown in a cross section through the 1301-N LWDF (Figure 22a). When the plume encounters the unconfined aquifer, the plume spreads laterally in both directions (Figure 22b and 22c) until the year 1983, when part of the liquid effluent discharged to the 1301-N LWDF was diverted to the 1325-N LWDF. The effects of this split in effluent discharge are seen in Figure 22d, as evidenced by streamline "A." The flow from the 1301-N LWDF in this plane is diverted upward toward the vadose zone. Although this streamline indicates that water is moving upward into the vadose zone, the velocity component in the third direction (X) was not used in calculating this streamline. Consequently, the path of water movement would actually be out of the plane, rather than upward, because the X and Y components of velocity are much larger than the Z component of velocity.

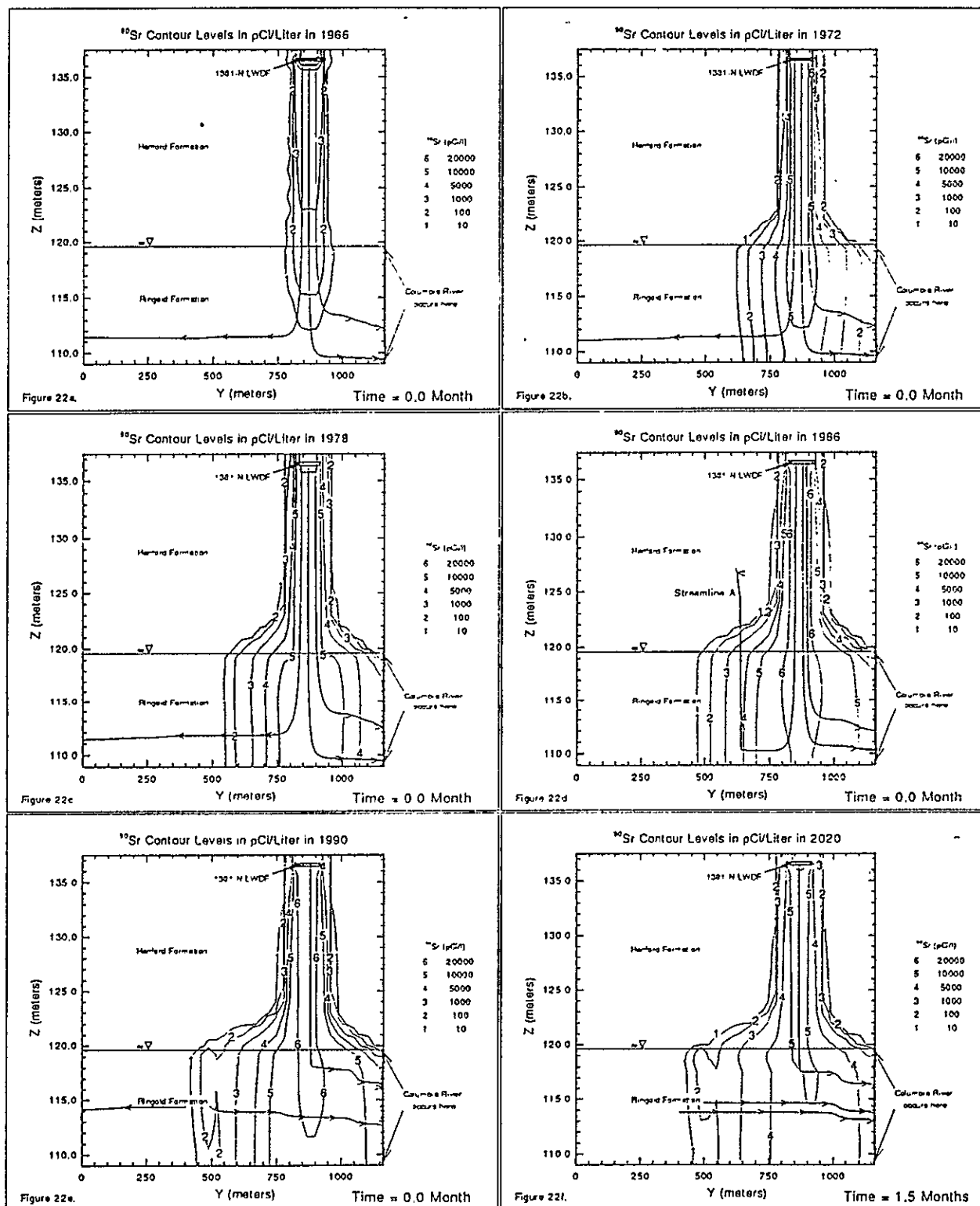


Figure 22. Selected Time-Dependent PORFLO-3 Results Showing the Downward and Outward Growth of the ^{90}Sr Plume Beneath the 1301-N Liquid Waste Disposal Facility.

The effect of all effluent flow being discharged to the 1325-N LWDF is to push the contaminant plume beneath the 1301-N LWDF toward the Columbia River. This effect can be seen in the streamlines of Figure 22e. After effluent discharges to the LWDFs have ceased, the movement of the ^{90}Sr plume will be toward the Columbia River (Figure 22f) at a rate equal to the velocity determined by the unperturbed steady-state flow field times the retardation coefficient. In Figures 21e through 21f, ^{90}Sr concentration levels 4, 5, and 6 have receded. This effect is attributable to radioactive decay once the source has been removed.

Figure 23 shows the areal distribution of the ^{90}Sr plume at the beginning of 1972, 1978, 1984, 1990, 2005, and 2020 (Figures 23a through 23f). The plume moved radially outward from the 1301-N LWDF from 1964 to 1983. Shortly after the start of operations for the 1325-N LWDF, a lobe of the plume developed beneath the 1325-N LWDF after discharges to that facility commenced (Figure 23c). The ^{90}Sr plume beneath the 1325-N LWDF continued to grow from 1983 to 1990. However, by 1986, all flows to the 1301-N LWDF ceased and the plume beneath the 1301-N LWDF had stabilized. This plume seems to have been relatively unaffected by the amount of effluent discharged to either the 1324 N/NA or 1325-N LWDFs. The reason for this apparent stability is the relatively high retardation coefficient (100) used in the simulation. Without additional discharges to the LWDFs, the plume should remain where it currently is and decay with time (Figures 23e through 23f).

As can be seen in Figure 22b, the leading edge of the ^{90}Sr plume began to arrive at the Columbia River in 1972. Starting in 1972, the simulation-predicted concentrations of ^{90}Sr at the Columbia River were monitored by the PORFLO-3 software. These concentrations at each time were multiplied by the simulated outflux of water to the river to calculate instantaneous and cumulative fluxes of ^{90}Sr entering the river. These fluxes were then used in the following section to estimate exposures of ^{90}Sr from the 100-N Area LWDFs to humans.

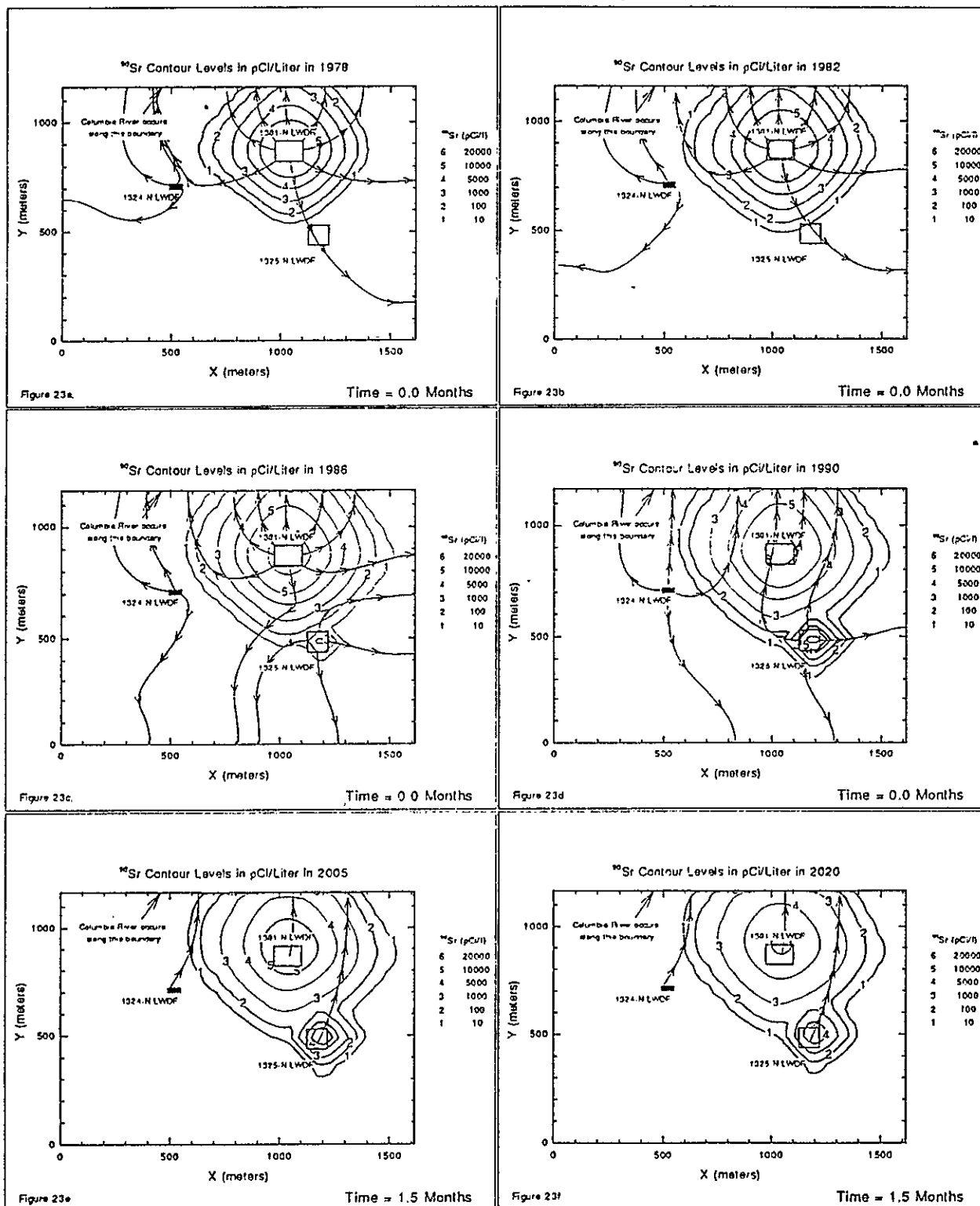


Figure 23. Selected Time-Dependent PORFLO-3 Results Showing the Area Extent of the ^{90}Sr Plume in the Unconfined Aquifer.

7.0 RADIATION DOSE FROM ^{90}Sr RELEASED FROM THE 100-N AREA LWDFs THAT ENTERS THE COLUMBIA RIVER AT N SPRINGS

Once the ^{90}Sr from the 100-N Area LWDFs has entered the Columbia River, it can be incorporated into foods eaten by humans. The main source of such contamination would be by irrigation of downstream farmland with water pumped from the Columbia River. Irrigation of this type currently occurs in the Riverview area, west of Pasco. The GENII program, Version 1.485 (Napier et al. 1988) was used to calculate the potential amount of radiation to humans.

7.1 ANNUAL RATE OF ^{90}Sr DISCHARGE TO THE COLUMBIA RIVER

The result from the PORFLO-3 simulations that was used to estimate the resultant radiation to humans for this report was the total annual flux at the Columbia River boundary (Figure 7) as a function of time. These data, shown in Table 8, were used to calculate the amounts of ^{90}Sr entering the Columbia River each year. The year-to-year difference in total annual flux is the amount of ^{90}Sr that entered the Columbia River that year.

Differences between releases calculated by PORFLO-3 and reported releases can be seen in Figure 24. Reported releases are calculated by taking the observed concentration at N Springs and multiplying it by a flux of water equal to 50% of the effluent discharged to 1301-N and 1325-N LWDFs. The differences between PORFLO-3 predicted flux and reported flux can be explained by the following: PORFLO-3 predicted the arrival of the plume before it was actually observed; once operations changed from the 1301-N LWDF to 1325-N LWDF, the 50% ratio of discharges to the LWDFs to discharges from the LWDFs at N Springs might be too large.

7.2 The ^{90}Sr PATHWAYS TO HUMANS

The pathways that were considered for exposing humans to radiation from water taken from the Columbia River that is contaminated by 100-N Area LWDF ^{90}Sr are as follows.

External Exposure Pathways:

- Ground contamination - deposited by irrigation water
- Recreation - swimming, boating, and shoreline activities.

Internal Exposure Pathways:

- Drinking water - most water from the Columbia River is treated before human consumption, but a small amount is ingested during aquatic recreation activities
- Aquatic foods - fish, mollusks, crustaceans, and aquatic plants

Table 8. Annual Discharges of ^{90}Sr to the Columbia River.
 From the 100-N Area Liquid Waste Disposal Facilities
 Via N Springs Estimated by the PORFLO-3 Software.

| Year | Discharge (Ci) | Year | Discharge (Ci) | Year | Discharge (Ci) |
|------|-------------------|------|-------------------|------|-------------------|
| 1964 | 0 | 1983 | 4.99 | 2002 | 0.840 |
| 1965 | 0 | 1984 | 4.93 | 2003 | 0.800 |
| 1966 | 0 | 1985 | 6.62 | 2004 | 0.800 |
| 1967 | 0 | 1986 | 5.03 | 2005 | 0.760 |
| 1968 | 1.20 E-05 | 1987 | 2.69 | 2006 | 0.580 |
| 1969 | 1.51 E-04 | 1988 | 1.95 | 2007 | 0.870 |
| 1970 | 0.00108 | 1989 | 1.56 | 2008 | 0.690 |
| 1971 | 0.00508 | 1990 | 1.44 | 2009 | 0.680 |
| 1972 | 0.0176 | 1991 | 1.17 | 2010 | 0.650 |
| 1973 | 0.0460 | 1992 | 1.19 | 2011 | 0.640 |
| 1974 | 0.103 | 1993 | 1.06 | 2012 | 0.610 |
| 1975 | 0.215 | 1994 | 0.890 | 2013 | 0.590 |
| 1976 | 0.404 | 1995 | 0.980 | 2014 | 0.600 |
| 1977 | 0.829 | 1996 | 0.870 | 2015 | 0.570 |
| 1978 | 1.573 | 1997 | 0.840 | 2016 | 0.560 |
| 1979 | 2.547 | 1998 | 0.810 | 2017 | 0.540 |
| 1980 | 3.727 | 1999 | 0.790 | 2018 | 0.530 |
| 1981 | 4.583 | 2000 | 0.770 | 2019 | 0.520 |
| 1982 | 5.29 | 2001 | 0.610 | 2020 | 0.510 |

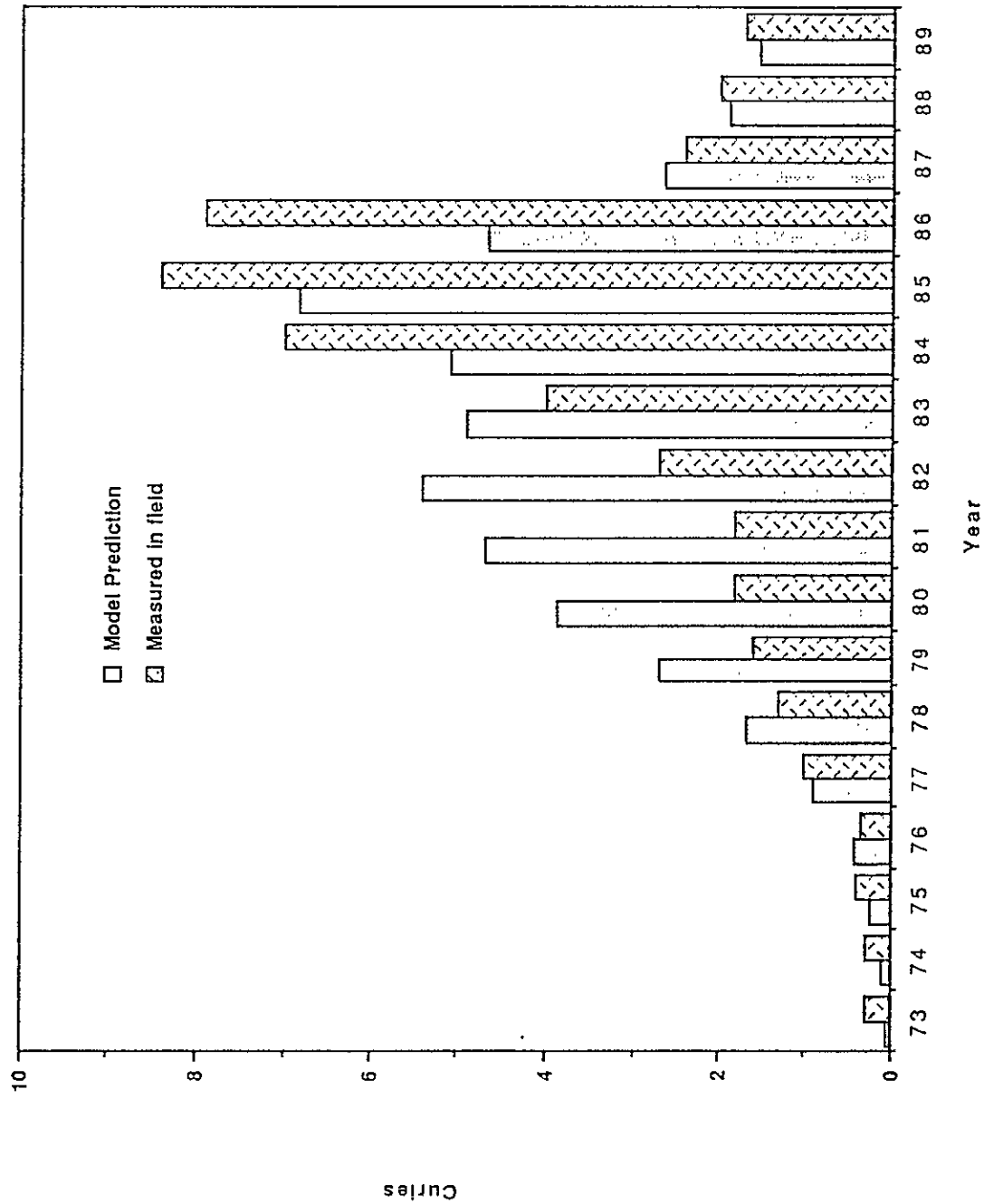


Figure 24. Comparison Between Annual Discharges of ^{90}Sr Calculated by PORFLO-3 to Reported Discharges for the Years 1973 Through 1989.

- Terrestrial foods - leafy and root vegetables, fruits, and grains contaminated by irrigation water from the Columbia River
- Animal products - beef and poultry, milk, and eggs; animals become contaminated by drinking contaminated water and eating contaminated vegetation and grain
- Inadvertent soil ingestion - assumed to be 0.41 g/d
- Inhalation of resuspended soil - determined using a mass-loading model.

7.3 DATA FILES USED BY GENII

The data files used by GENII are listed below. A sample input file for the GENII program is included as Appendix A for reference.

Data Files Used by GENII (Version 1.485):

| | |
|--|--|
| GENII Default Parameter Values | (28-Mar-90 RAP) |
| Radionuclide Master Library | (15-Nov-90 PDR) |
| Food Transfer Factor Library - | (RAP 29-Aug-88) (UPDATED LEACHING FACTORS) |
| Bioaccumulation Factor Library - | (30-Aug-88) RAP |
| External Dose Factors for GENII in person Sv/yr per Bq/n | (8-May-90 RAP) |
| Internal Dose Increments, Worst Case Solubilities, | 12/03/90 PDR |

7.4 COMPUTATION OF CUMULATIVE RADIATION COMMITMENTS

A small portion of the ^{90}Sr released to the Columbia River each year from the 100-N Area LWDFs is assumed to reach farmland via irrigation. Most of the human intake of ^{90}Sr would occur during the year as the irrigation occurs. However, some ^{90}Sr would remain in the soil and be taken up in food products in subsequent years. These phenomena can be simulated using the GENII computer program.

The length of the exposure to residual contamination (known as the intake period) was adjusted according to the number of years until the year 2034 (70 yr from the time of initial operation of the 1301-N LWDF). This year was arbitrarily selected and has little effect on the cumulative radiation received. The intake period would be 50 yr for irrigation in 1984 and 40 yr for irrigation in 1994.

The ^{90}Sr that is inhaled or ingested remains in the body for several years afterward, giving a decreasing amount of exposure each year as it gradually decays and is excreted. Current practice requires that the radiation an individual is committed to receive during the next 50 to 70 yr be credited as being received this year and then dropped from further consideration. A 70-yr period is used for this analysis. This 70-yr commitment period is used for all ^{90}Sr inhaled or ingested between 1964 and 2020.

The GENII program was not run for all 70 intake periods to find the cumulative mrem for curies released. Instead, it was run for 7 selected intake periods (2, 5, 10, 20, 30, 50, and 70 yr). The results were then approximated. The resultant data appeared to exponentially increase to a steady state; consequently, an equation of the form $a - b \cdot \text{EXP}(-c \cdot t)$ was used to fit the data to a curve, where "t" is the intake period. Values for "a", "b" and "c", and the differences between the results from the GENII program and the curve-fitting equation are shown in Table 9. The differences are sufficiently small to be concealed by rounding off to two significant digits and are not apparent when the results are graphically compared (Figures 25 and 26).

The equation used to approximate cumulative dose per curie of ^{90}Sr released as a function of intake duration is

$$\text{Dose} = a - b \cdot \text{EXP}(-c \cdot t)$$

where

| | |
|--------------|--------------|
| a = 6.97E-05 | a = 0.000708 |
| b = 3.61E-05 | b = 0.000375 |
| c = 0.0368 | c = 0.0393 |

Table 9. Comparison of GENII and Curve-Fitting Equation Results Cumulative Dose per Curie of ^{90}Sr Released.

| Intake period | Effective Dose Equivalent | | | Bone Surface (rem) | | |
|---------------|---------------------------|-----------|------------|--------------------|-----------|------------|
| | Curve-Fit | | | Curve-Fit | | |
| | GENII | Equation | Difference | GENII | Equation | Difference |
| 1 | 3.5 E-05 | 3.49 E-05 | -0.27% | 3.5 E-04 | 3.47 E-04 | -0.73% |
| 2 | 3.6 E-05 | 3.62 E-05 | 0.45% | 3.6 E-04 | 3.61 E-04 | 0.37% |
| 5 | 4.0 E-05 | 3.97 E-05 | -0.83% | 4.0 E-04 | 4.00 E-04 | -0.03% |
| 10 | 4.5 E-05 | 4.47 E-05 | -0.63% | 4.5 E-04 | 4.55 E-04 | 1.08% |
| 20 | 5.2 E-05 | 5.24 E-05 | 0.78% | 5.4 E-04 | 5.37 E-04 | -0.53% |
| 30 | 5.8 E-05 | 5.77 E-05 | -0.46% | 5.9 E-04 | 5.93 E-04 | 0.45% |
| 50 | 6.4 E-05 | 6.40 E-05 | -0.05% | 6.6 E-04 | 6.55 E-04 | -0.69% |
| 70 | 6.7 E-05 | 6.70 E-05 | -0.07% | 6.8 E-04 | 6.84 E-04 | 0.60% |

Using the equation noted above, the doses shown in Tables 10 and 11 were computed. The annual dose from ^{90}Sr is the product of the amount of ^{90}Sr released to the Columbia River that year and the dose per unit amount of ^{90}Sr released as approximated by the above equation. The intake period used in the above equation is the difference between the year 2034 and the current year.

Figure 27 is provided for reference. It shows the annual and cumulative releases of ^{90}Sr to the Columbia River from the 100-N Area LWDFs. Figure 28 shows the resultant annual and cumulative dose in terms of the effective dose equivalent (EDE). Dose to the surface of the bones of an exposed individual was determined to be very nearly 10 times the EDE (not shown).

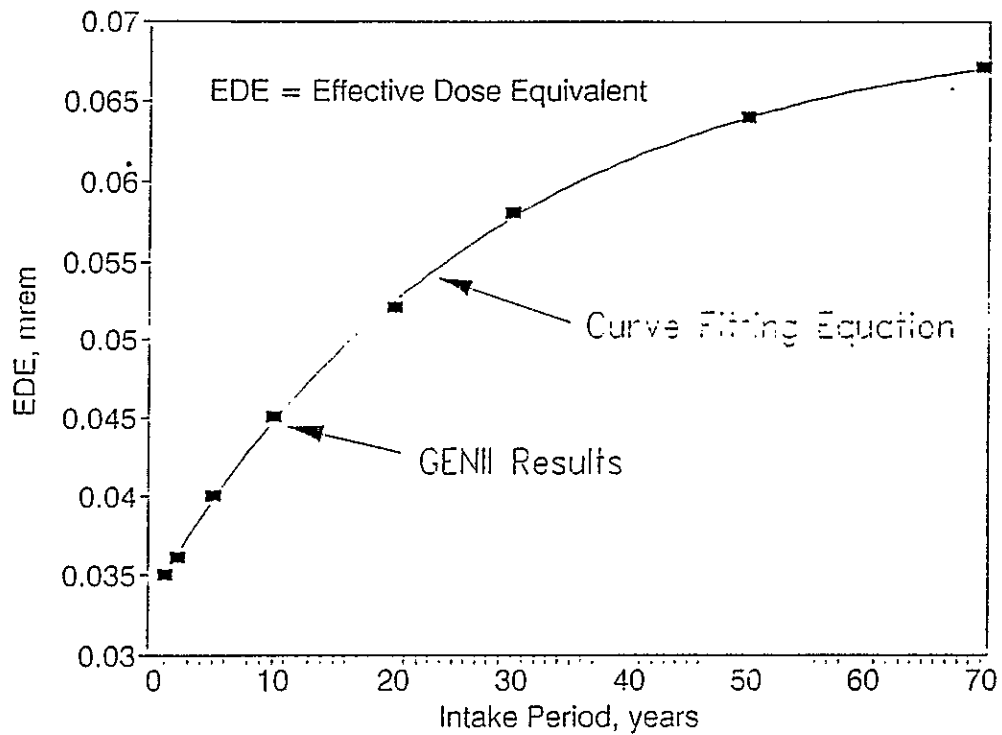


Figure 25. Comparison of Effective Dose Equivalents Generated by GENII and the Curve-Fitting Equation.

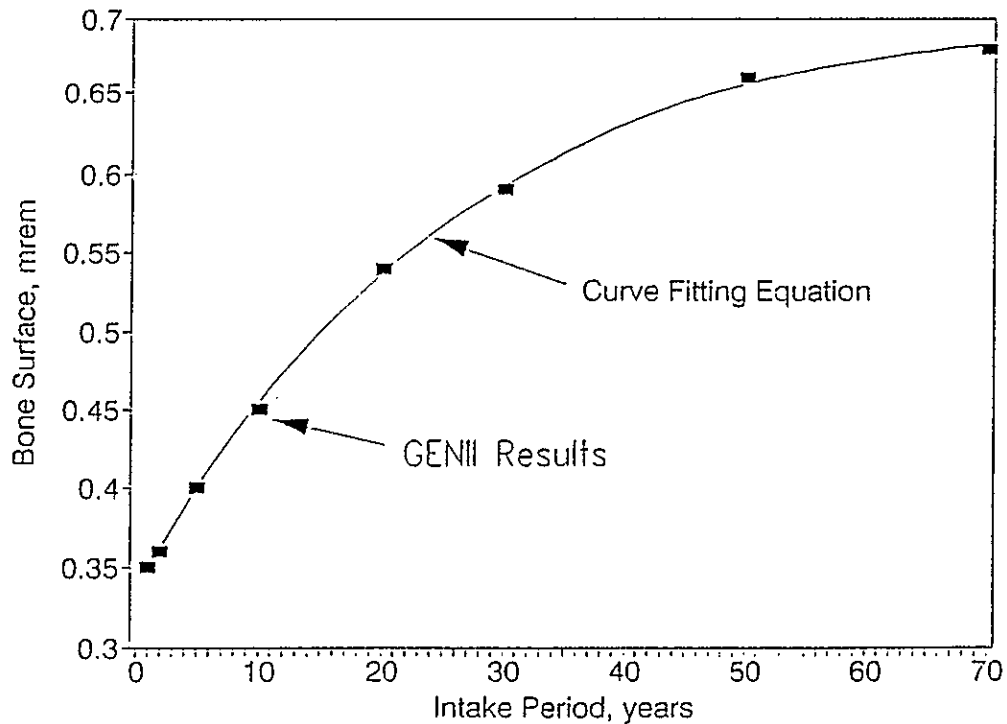


Figure 26. Comparison of Bone Dose Calculated Using GENII and the Curve-Fitting Equation.

Table 10. Seventy-Year Effective Dose Equivalent (mrem).

| Year | Years of Intake | Annual Dose | Cumulative Dose | Year | Years of Intake | Annual Dose | Cumulative Dose |
|------|-----------------|-------------|-----------------|------|-----------------|-------------|-----------------|
| 1964 | 70 | 0.0 E+00 | 0.0 E+00 | 1993 | 41 | 6.5 E-02 | 3.3 E+00 |
| 1965 | 69 | 0.0 E+00 | 0.0 E+00 | 1994 | 40 | 5.5 E-02 | 3.4 E+00 |
| 1966 | 68 | 0.0 E+00 | 0.0 E+00 | 1995 | 39 | 6.0 E-02 | 3.4 E+00 |
| 1967 | 67 | 0.0 E+00 | 0.0 E+00 | 1996 | 38 | 5.3 E-02 | 3.5 E+00 |
| 1968 | 66 | 8.0 E-07 | 8.0 E-07 | 1997 | 37 | 5.1 E-02 | 3.5 E+00 |
| 1969 | 65 | 1.0 E-05 | 1.1 E-05 | 1998 | 36 | 4.9 E-02 | 3.6 E+00 |
| 1970 | 64 | 7.2 E-05 | 8.2 E-05 | 1999 | 35 | 4.7 E-02 | 3.6 E+00 |
| 1971 | 63 | 3.4 E-04 | 4.2 E-04 | 2000 | 34 | 4.6 E-02 | 3.7 E+00 |
| 1972 | 62 | 1.2 E-03 | 1.6 E-03 | 2001 | 33 | 3.6 E-02 | 3.7 E+00 |
| 1973 | 61 | 3.0 E-03 | 4.6 E-03 | 2002 | 32 | 4.9 E-02 | 3.8 E+00 |
| 1974 | 60 | 6.7 E-03 | 1.1 E-02 | 2003 | 31 | 4.7 E-02 | 3.8 E+00 |
| 1975 | 59 | 1.4 E-02 | 2.5 E-02 | 2004 | 30 | 4.6 E-02 | 3.9 E+00 |
| 1976 | 58 | 2.6 E-02 | 5.2 E-02 | 2005 | 29 | 4.4 E-02 | 3.9 E+00 |
| 1977 | 57 | 5.4 E-02 | 1.1 E-01 | 2006 | 28 | 3.3 E-02 | 3.9 E+00 |
| 1978 | 56 | 1.0 E-01 | 2.1 E-01 | 2007 | 27 | 4.9 E-02 | 4.0 E+00 |
| 1979 | 55 | 1.7 E-01 | 3.7 E-01 | 2008 | 26 | 3.9 E-02 | 4.0 E+00 |
| 1980 | 54 | 2.4 E-01 | 6.2 E-01 | 2009 | 25 | 3.8 E-02 | 4.1 E+00 |
| 1981 | 53 | 3.0 E-01 | 9.1 E-01 | 2010 | 24 | 3.6 E-02 | 4.1 E+00 |
| 1982 | 52 | 3.4 E-01 | 1.3 E-00 | 2011 | 23 | 3.5 E-02 | 4.1 E+00 |
| 1983 | 51 | 3.2 E-01 | 1.6 E-00 | 2012 | 22 | 3.3 E-02 | 4.2 E+00 |
| 1984 | 50 | 3.2 E-01 | 1.9 E-00 | 2013 | 21 | 3.1 E-02 | 4.2 E+00 |
| 1985 | 49 | 4.2 E-01 | 2.3 E-00 | 2014 | 20 | 3.1 E-02 | 4.2 E+00 |
| 1986 | 48 | 3.2 E-01 | 2.6 E-00 | 2015 | 19 | 3.0 E-02 | 4.3 E+00 |
| 1987 | 47 | 1.7 E-01 | 2.8 E-00 | 2016 | 18 | 2.9 E-02 | 4.3 E+00 |
| 1988 | 46 | 1.2 E-01 | 2.9 E-00 | 2017 | 17 | 2.7 E-02 | 4.3 E+00 |
| 1989 | 45 | 9.8 E-02 | 3.0 E-00 | 2018 | 16 | 2.6 E-02 | 4.3 E+00 |
| 1990 | 44 | 9.0 E-02 | 3.1 E-00 | 2019 | 15 | 2.5 E-02 | 4.4 E+00 |
| 1991 | 43 | 7.3 E-02 | 3.2 E-00 | 2020 | 14 | 2.5 E-02 | 4.4 E+00 |
| 1992 | 42 | 7.4 E-02 | 3.3 E-00 | | | | |

Table 11. Seventy-Year Dose to the Bone Surface (mrem).

| Year | Years of Intake | Annual Dose | Cumulative Dose | Year | Years of Intake | Annual Dose | Cumulative Dose |
|------|-----------------|-------------|-----------------|------|-----------------|-------------|-----------------|
| 1964 | 70 | 0.0 E+00 | 0.0 E+00 | 1993 | 41 | 6.7 E-01 | 3.4 E+01 |
| 1965 | 69 | 0.0 E+00 | 0.0 E+00 | 1994 | 40 | 5.6 E-01 | 3.5 E+01 |
| 1966 | 68 | 0.0 E+00 | 0.0 E+00 | 1995 | 39 | 6.1 E-01 | 3.5 E+01 |
| 1967 | 67 | 0.0 E+00 | 0.0 E+00 | 1996 | 38 | 5.4 E-01 | 3.6 E+01 |
| 1968 | 66 | 8.2 E-06 | 8.2 E-06 | 1997 | 37 | 5.2 E-01 | 3.6 E+01 |
| 1969 | 65 | 1.0 E-04 | 1.1 E-04 | 1998 | 36 | 5.0 E-01 | 3.7 E+01 |
| 1970 | 64 | 7.3 E-04 | 8.4 E-04 | 1999 | 35 | 4.8 E-01 | 3.7 E+01 |
| 1971 | 63 | 3.4 E-03 | 4.3 E-03 | 2000 | 34 | 4.7 E-01 | 3.8 E+01 |
| 1972 | 62 | 1.2 E-02 | 1.6 E-02 | 2001 | 33 | 3.7 E-01 | 3.8 E+01 |
| 1973 | 61 | 3.1 E-02 | 4.7 E-02 | 2002 | 32 | 5.1 E-01 | 3.9 E+01 |
| 1974 | 60 | 6.9 E-02 | 1.2 E-01 | 2003 | 31 | 4.8 E-01 | 3.9 E+01 |
| 1975 | 59 | 1.4 E-01 | 2.6 E-01 | 2004 | 30 | 4.7 E-01 | 4.0 E+01 |
| 1976 | 58 | 2.7 E-01 | 5.3 E-01 | 2005 | 29 | 4.5 E-01 | 4.0 E+01 |
| 1977 | 57 | 5.5 E-01 | 1.1 E+00 | 2006 | 28 | 3.4 E-01 | 4.0 E+01 |
| 1978 | 56 | 1.0 E+00 | 2.1 E+00 | 2007 | 27 | 5.0 E-01 | 4.1 E+01 |
| 1979 | 55 | 1.7 E+00 | 3.8 E+00 | 2008 | 26 | 4.0 E-01 | 4.1 E+01 |
| 1980 | 54 | 2.5 E+00 | 6.3 E+00 | 2009 | 25 | 3.9 E-01 | 4.2 E+01 |
| 1981 | 53 | 3.0 E+00 | 9.3 E+00 | 2010 | 24 | 3.7 E-01 | 4.2 E+01 |
| 1982 | 52 | 3.5 E+00 | 1.3 E+01 | 2011 | 23 | 3.6 E-01 | 4.2 E+01 |
| 1983 | 51 | 3.3 E+00 | 1.6 E+01 | 2012 | 22 | 3.4 E-01 | 4.3 E+01 |
| 1984 | 50 | 3.2 E+00 | 1.9 E+01 | 2013 | 21 | 3.2 E-01 | 4.3 E+01 |
| 1985 | 49 | 4.3 E+00 | 2.4 E+01 | 2014 | 20 | 3.2 E-01 | 4.3 E+01 |
| 1986 | 48 | 3.3 E+00 | 2.7 E+01 | 2015 | 19 | 3.0 E-01 | 4.4 E+01 |
| 1987 | 47 | 1.7 E+00 | 2.9 E+01 | 2016 | 18 | 2.9 E-01 | 4.4 E+01 |
| 1988 | 46 | 1.3 E+00 | 3.0 E+01 | 2017 | 17 | 2.8 E-01 | 4.4 E+01 |
| 1989 | 45 | 1.0 E+00 | 3.1 E+01 | 2018 | 16 | 2.7 E-01 | 4.4 E+01 |
| 1990 | 44 | 9.2 E-01 | 3.2 E+01 | 2019 | 15 | 2.6 E-01 | 4.5 E+01 |
| 1991 | 43 | 7.5 E-01 | 3.3 E+01 | 2020 | 14 | 2.5 E-01 | 4.5 E+01 |
| 1992 | 42 | 7.6 E-01 | 3.3 E+01 | | | | |

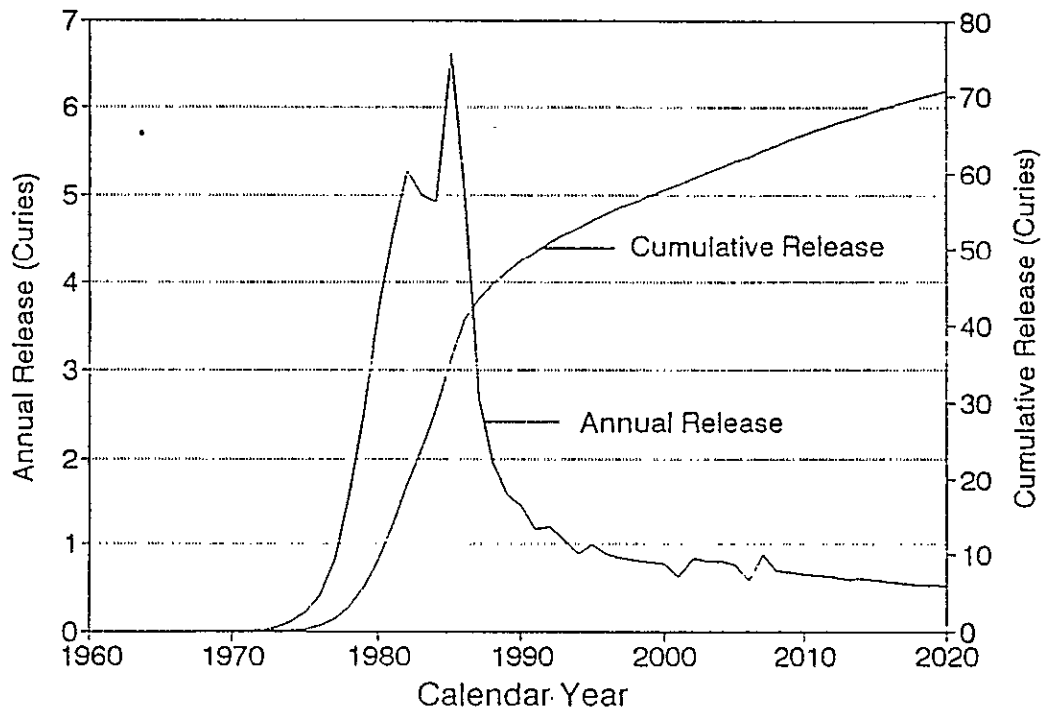


Figure 27. Annual and Cumulative Releases of ^{90}Sr from the 100-N Area Liquid Waste Disposal Facility to the Columbia River.

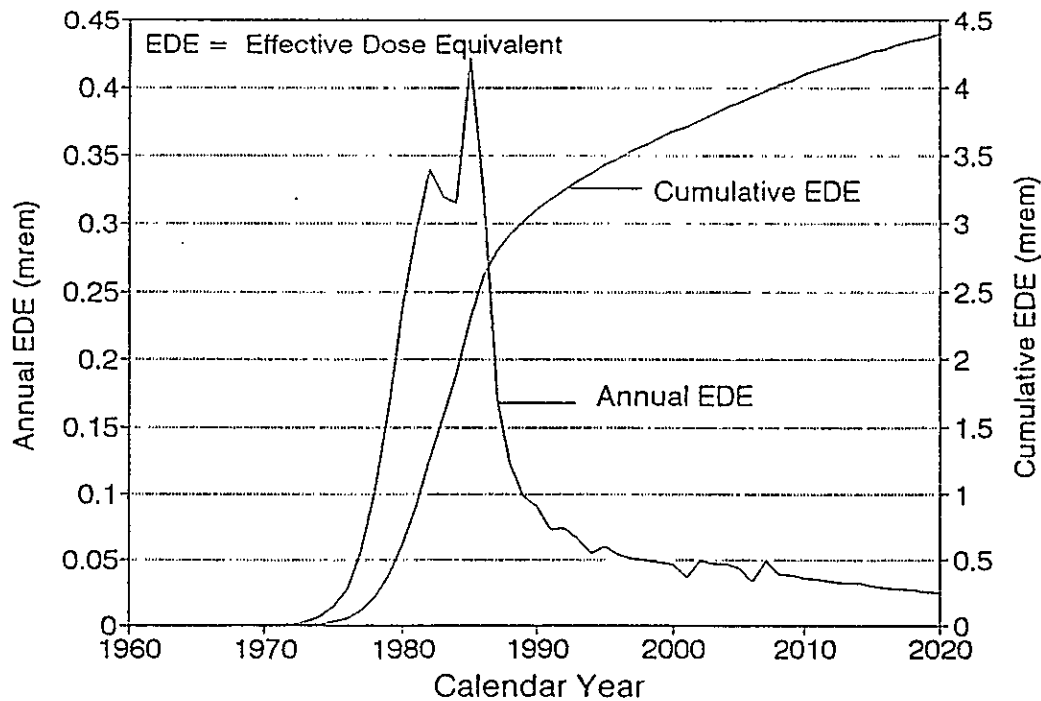


Figure 28. Annual and Cumulative Doses from ^{90}Sr Released from the 100-N Area Liquid Waste Disposal Facilities (Effective Dose Equivalent).

For comparison with regulatory limits, the method used in the annual environmental reports generated by Pacific Northwest Laboratory is more appropriate than the cumulative method used above. In this method assumed in the regulations, the effects of residual contamination are ignored. In Figures 29 and 30 the doses from both methods are shown. For ^{90}Sr , the effect of omitting the residual contamination is to halve the projected doses. Since the doses from the full model are well below the regulatory limit of 25 mrem/yr (and, beginning in 1991, 10 mrem/yr), the doses computed using the standard model also are far below the limits.

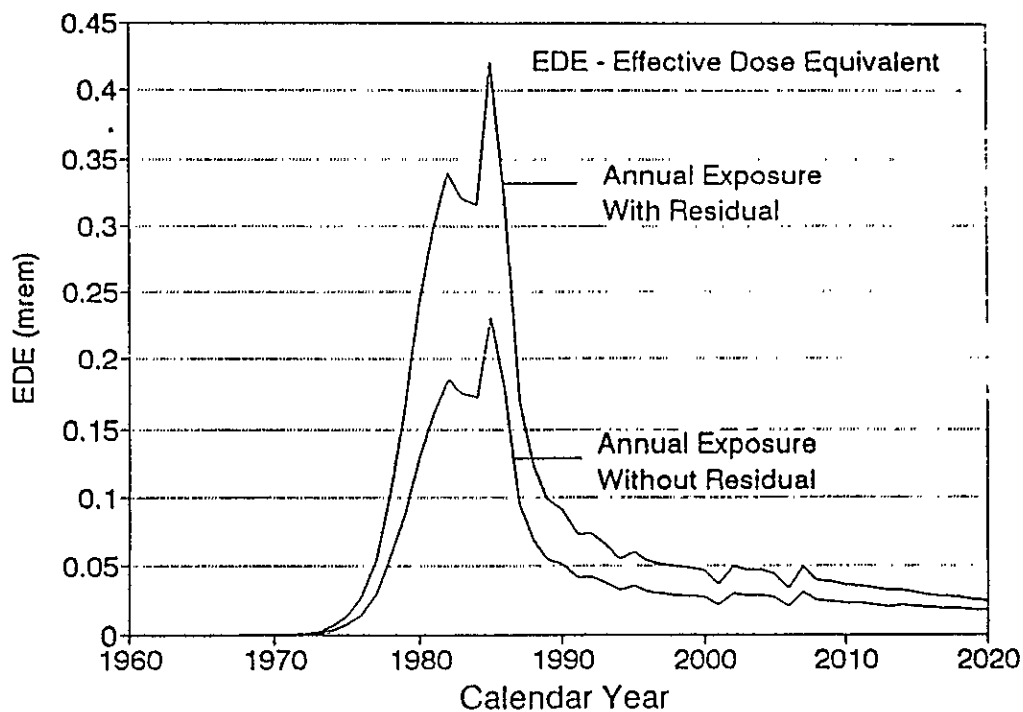


Figure 29. The Effect of Residual Contamination on Computation of Annual Exposures.

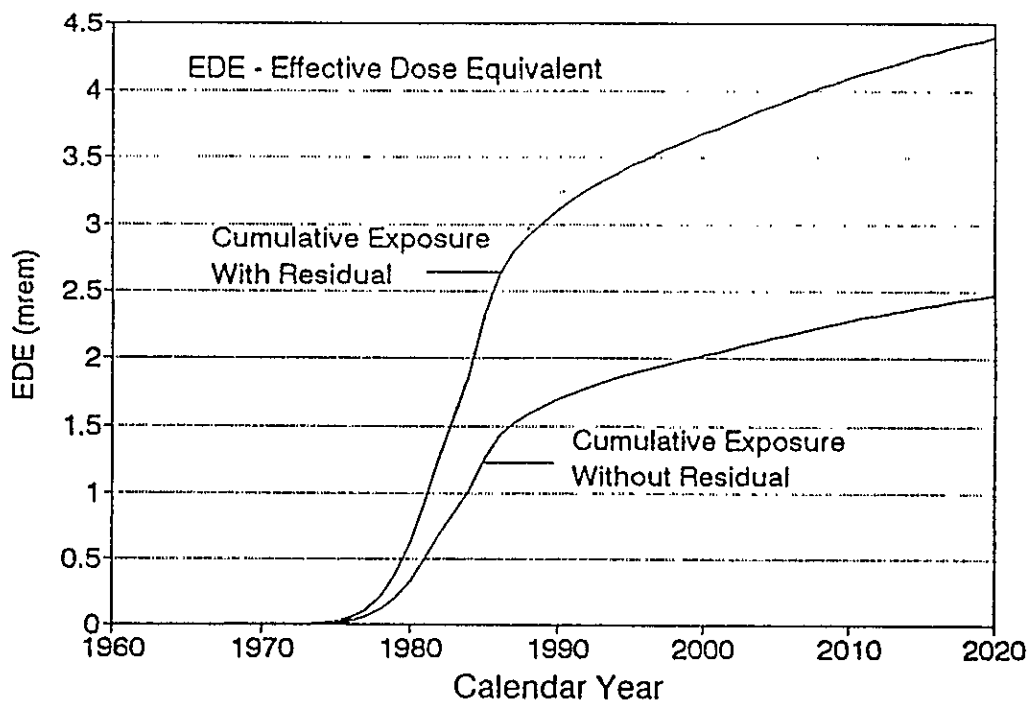


Figure 30. The Effect of Residual Contamination on Computation of Cumulative Exposures.

9513381-0074

WHC-SD-ER-TA-001

This page intentionally left blank.

8.0 SUMMARY AND RECOMMENDATIONS

A three-dimensional simulation was made of groundwater movement in the vadose zone and the unconfined aquifer, and the movement of ^{90}Sr in that groundwater using a computer-encoded numerical model. The simulation approximated how groundwater beneath the 100-N Area has responded to the disposal of liquid effluents containing ^{90}Sr . During the analysis, it became evident that there were inconsistencies and large variabilities in the groundwater and contaminant transport data for the 100-N Area. The inconsistencies highlight what data is needed and where it should be collected.

Examples of such data inconsistencies and variability include, but are not limited to, the following.

- Reported hydraulic conductivities for the unconfined aquifer in the 100-N Area vary by as much as five times.
- Discrepancies exist between the hydraulic conductivity based on the arrival time of ^{131}I at N Springs (Crews and Tillson 1969) and the observed height of water-table mounding beneath the LWDFs.
- An arbitrarily high sorption coefficient had to be assigned for the conceptual model used by this analysis to the layer at the bottom of the LWDFs and the underlying sediments to reconcile the extent and concentration of the ^{90}Sr contamination to what was observed by earlier studies at N Springs.

Based on the results of this analysis, we conclude that the vadose zone and the layer at the bottom of cribs play a critical role in determining the movement of ^{90}Sr to the unconfined aquifer. Consequently, the following data should be collected: (1) sorption coefficients for ^{90}Sr , (2) moisture characteristic curves, and (3) moisture contents for the sludge layer and sediments directly beneath the 1301-N LWDF. A large number of samples is not needed to obtain these data; three or four samples at the bottom of the 1301-N LWDF are likely to suffice.

In addition, when discharges of liquid effluents to the LWDFs cease, the steady-state hydraulic gradient must be determined to calculate groundwater velocities which, in turn, can be used to estimate the rate of transport of contaminants. A better estimate of horizontal hydraulic conductivities in the unconfined aquifer also is needed. Because of the problems associated with disposal of the contaminated purgewater from pump tests, consideration should be given to determining the needed hydraulic conductivities based on the observed relationship between the water levels in monitoring wells and the elevation of the Columbia River.

9513381.0076

WHC-SD-ER-TA-001

This page intentionally left blank.

9.0 REFERENCES

- ANSI/ASME, 1983, *Quality Assurance Program Requirements for Nuclear Facilities*, NQA-1-1983, American National Standards Institute and American Society of Mechanical Engineers, New York, New York.
- Baker, V. R., 1973, *Paleohydrology and Sedimentology of the Lake Missoula Flooding in Eastern Washington*, Geological Society of America, Special Paper 144, Boulder, Colorado.
- Bjornstad, B. N., 1984, *Suprabasalt Stratigraphy Within and Adjacent to the Reference Repository Location*, SD-BWI-DP-039, Rockwell Hanford Operations, Richland, Washington.
- Bjornstad, B. N., 1985, *Late Cenozoic Stratigraphy and Tectonic Evolution Within a Subsiding Basin, South-Central Washington*, RHO-BW-SA-478P, Rockwell Hanford Operations, Richland, Washington.
- Bretz, J. H., 1959, *Washington's Channeled Scabland*, Washington Division of Mines and Geology Bulletin 45, Olympia, Washington.
- Brown, D. J., 1962, *Geology Underlying Hanford Reactor Areas*, HW-69571, General Electric Company, Hanford Atomic Products Operation, Richland, Washington.
- Brown, D. J., 1964, *Groundwater Travel Time Calculations for the 1301-N Crib*, HW-80558, General Electric Company, Hanford Atomic Products Operation, Richland, Washington.
- Brown, R. E., 1975, *Groundwater and the Basalts in the Pasco Basin*, Proceedings of the Thirteenth Engineering Geology and Soils Engineering Symposium, April 2-4, 1975, Moscow, Idaho.
- Brown, D. J. and P. P. Rowe, 1960, *100-N Area Aquifer Evaluation*, HW-6736, General Electric Company, Hanford Atomic Products Operation, Richland, Washington.
- Crews, W. S. and D. D. Tillson, 1969, *Analysis of Travel Time of I-131 from the 1301-N Crib to the Columbia River During July 1969*, BNWL-CC-2326, Pacific Northwest Laboratory, Richland, Washington.
- Cucchiara A. L., 1975, *UNC Nuclear Industries Reactor and Fuels Production Facilities 1974 Effluent Release Report*, UNI-2358, United Nuclear Industries, Inc., Richland, Washington.
- Cucchiara A. L., 1976, *UNC Nuclear Industries Reactor and Fuels Production Facilities 1975 Effluent Release Report*, UNI-2358, United Nuclear Industries, Inc., Richland, Washington.
- Cucchiara A. L., 1977, *UNC Nuclear Industries Reactor and Fuels Production Facilities 1976 Effluent Release Report*, UNI-2358, United Nuclear Industries, Inc., Richland, Washington.

- Cucchiara A. L., 1978, *UNC Nuclear Industries Reactor and Fuels Production Facilities 1977 Effluent Release Report*, UNI-2358, United Nuclear Industries, Inc., Richland, Washington.
- De Marsily, G., 1986, *Quantitative Hydrology -- Groundwater Hydrology for Engineers*, Academic Press, Harcourt Brace Jovanovich, Publishers, Orlando, Florida.
- DOE, 19 , *Radiation Protection of the Public and the Environment*, DOE Order 5400.5, U.S. Department of Energy, Washington, D.C.
- DOE, 1987, *Closure Plan, 1324-NA Percolation Pond*, Rev. 0, U.S. Department of Energy, Washington, D.C.
- Ecology, EPA, and DOE, 1989, *Hanford Federal Facility Agreement and Consent Order*, Washington State Department of Ecology, U.S. Environmental Protection Agency, and U.S. Department of Energy, Olympia, Washington.
- WHC, 1988, *Standard Engineering Practices*, WHC-CM-6-6, Westinghouse Hanford Company, Richland, Washington.
- Flint, R. F., 1938, *Origin of the Cheney-Palouse Scabland Tract*, Geological Society of America Bulletin 49, pp. 461-524.
- Fogel, P. A., 1983, *UNC Nuclear Industries Reactor and Fuels Production Facilities 1982 Effluent Release Report*, UNI-2358, United Nuclear Industries, Inc., Richland, Washington.
- Gephardt, R. E., R. C. Arnett, R. G. Baca, L. S. Leonhart, and F. A. Spane, Jr., 1979, *Hydrologic Studies Within the Columbia Plateau, Washington: An Integration of Current Knowledge*, RHO-BWI-ST-5, Rockwell Hanford Operations, Richland, Washington.
- Gilmore, T. J., J. V. Borghese, J. P. McDonald, and D. R. Newcomer, 1990, *Evaluations of the Effects of the Columbia River on the Unconfined Aquifer Beneath the 1301-N Liquid Waste Disposal Facility*, PNL-7341, Pacific Northwest Laboratory, Richland, Washington.
- Greager, E. M., 1979, *UNC Nuclear Industries, Inc., Reactor and Fuels Production Facilities 1978 Effluent Release Report*, UNI-1261, United Nuclear Industries Inc., Richland, Washington.
- Greager, E. M., 1980, *UNC Nuclear Industries, Inc., Reactor and Fuels Production Facilities 1979 Effluent Release Report*, UNI-1474, United Nuclear Industries, Inc., Richland, Washington.
- Greager, E. M., 1981, *UNC Nuclear Industries, Inc., Reactor and Fuels Production Facilities 1980 Effluent Release Report*, UNI-1701, United Nuclear Industries, Inc., Richland, Washington.
- Hajek, B. F., 1968, *Waste Disposal to the Ground at 100-N*, BNWL-CC-1670, Pacific Northwest Laboratory, Richland, Washington.

- Lu, A. H., 1990, *Simulations of ^{90}Sr Transport from the 100-N Area to the Columbia River Using VAM2DH*, WHC-EP-0369, Westinghouse Hanford Company, Richland, Washington.
- Napier, B. A., R. A. Peloquin, D. L. Strenge, J. V. Ramsdell, 1988, *GENII - The Hanford Environmental Radiation Dosimetry Software System, Volume 2: Users' Manual*, PNL-6584, Pacific Northwest Laboratory, Richland, Washington.
- Perkins, C. J., 1988, *Westinghouse Hanford Company Environmental Surveillance Annual Report--100 Areas, Calendar Year 1987*, WHC-EP-0161, Westinghouse Hanford Company, Richland, Washington.
- Perkins, C. J., 1989, *Characterization of Radionuclide Concentrations Along the N Springs Shoreline for 1988*, WHC-SP-0480, Westinghouse Hanford Company, Richland, Washington.
- Prater, L. S., 1984, *Groundwater Surveillance at the Hanford Site for Calendar Year 1983*, PNL-5041, Pacific Northwest Laboratory, Richland, Washington.
- Pratt, D. R., 1984, *Engineering Study: Liquid Effluent Disposal Facility Project H-672*, UNI-2999, United Nuclear Industries, Inc., Richland, Washington.
- Rohay, V. J., 1990, *Liquid Effluent Study Project Plan*, WHC-EP-0275, Revision 2, Westinghouse Hanford Company, Richland, Washington.
- Rokkan, D. J., 1984, *UNC Nuclear Industries Reactor and Fuels Production Facilities 1983 Effluent Release Report*, UNI-2795, United Nuclear Industries, Inc., Richland, Washington.
- Rokkan, D. J., 1985, *UNC Nuclear Industries Reactor and Fuels Production Facilities 1984 Effluent Release Report*, UNI-3284, United Nuclear Industries, Inc., Richland, Washington.
- Rokkan, D. J., 1987, *UNC Nuclear Industries Reactor and Fuel Production Facilities 1986 Effluent Release Report*, WHC-EP-0088, Westinghouse Hanford Company, Richland, Washington.
- Rokkan, D. J., 1988, *Westinghouse Hanford Company 100 Areas Environmental Releases for 1987*, WHC-EP-0165, Westinghouse Hanford Company, Richland, Washington.
- Routson, R. C. and K. R. Fecht, 1979, *Soil (Sediment) Properties of Twelve Hanford Wells with Geologic Interpretation*, RHO-LD-82, Rockwell Hanford Operations, Richland, Washington.
- Runchal, A. K. and B. Sagar, 1989, *PORFLO-3: A Mathematical Model for Fluid Flow, Heat, and Mass Transport in Variably Saturated Geologic Media, Users Manual - Version 1.0*, WHC-EP-0041, Westinghouse Hanford Company, Richland, Washington.

- Sagar, B., and A. K. Runchal, 1989, *PORFLO-3: A Mathematical Model for Fluid Flow, Heat, and Mass Transport in Variably Saturated Geologic Media, Theory - Version 1.0*, WHC-EP-0042, Westinghouse Hanford Company, Richland, Washington.
- Skaags, R. W. and R. Khaleel, 1982, "Infiltration," *Hydrologic Modeling of Small Watersheds*, C.T. Haan, editor, American Society of Agricultural Engineers Monograph 5, American Society of Agricultural Engineers, St. Joseph, Missouri.
- Tallman, A. M., K. R. Fecht, M. C. Marratt, and G. V. Last, 1979, *Geology of the Separation Areas, Hanford Site, South-Central, Washington*, RHO-ST-23, Rockwell Hanford Operations, Richland, Washington.
- Van Genuchten, M. Th., 1985, *Program to Analyze Observed Soil Water Tension and Hydraulic Conductivity Data*, U.S. Salinity Laboratory, Special Report, Riverside, California.
- Waite, R. B., Jr., 1980, "About Forth Last-Glacial Lake Missoula Jokulhlaups Through Southern Washington," *Journal of Geology*, Vol. 88, pp. 653-679.

9513381.0081

WHC-SD-ER-TA-001

APPENDIX

PROGRAM GENII INPUT FILE

9613381.0082

WHC-SD-ER-TA-001

This page intentionally left blank.

Program GENII Input File ##### 8 Jul 88

Title: Routine Discharge to the Columbia River

\R30.IN

Created on 07-26-1990 at 09:28

OPTIONS===== Default =====

F Near-field scenario? (Far-field) NEAR-FIELD: narrowly-focused
 F Population dose? (Individual) release, single site
 F Acute release? (Chronic) FAR-FIELD: wide-scale release,
 Maximum Individual data set used multiple sites

Complete
 TRANSPORT OPTIONS===== Section EXPOSURE PATHWAY OPTIONS===== Section

F Air Transport 1 F Finite plume, external 5
 T Surface Water Transport 2 F Infinite plume, external 5
 F Biotic Transport (near-field) 3,4 T Ground, external 5
 F Waste Form Degradation (near) 3,4 T Recreation, external 5
 T Inhalation uptake 5,6
 T Drinking water ingestion 7,8
 T Aquatic foods ingestion 7,8
 T Terrestrial foods ingestion 7,9
 T Animal product ingestion 7,10
 T Inadvertent soil ingestion

REPORT OPTIONS=====

F Report AEDE only
 F Report by radionuclide
 T Report by exposure pathway
 F Debug report on screen

INVENTORY #####

- 4 Inventory input activity units: (1-pCi 2-uCi 3-mCi 4-Ci 5-Bq)
 0 Surface soil source units (1- m2 2- m3 3- kg)
 Equilibrium question goes here

| Use when | ---Release Terms--- | | | ---Basic Concentrations--- | | | | |
|---------------|---------------------|-----------|-----------|---------------------------------|------------|----------|----------|----------|
| | transport selected | | | near-field scenario, optionally | | | | |
| Release | Surface Buried | | | Surface Deep | | Ground | Surface | |
| Radio-nuclide | Air /yr | Water /yr | Waste /m3 | Air /m3 | Soil /unit | Soil /m3 | Water /L | Water /L |
| SR90 | | 1.0E+00 | | | | | | |
| Y 90 | | 1.0E+00 | | | | | | |

| Use when | ---Derived Concentrations--- | | | |
|---------------|------------------------------|----------------|-------------|--------------|
| | measured values are known | | | |
| Release | Terres. Plant | Animal Product | Drink Water | Aquatic Food |
| Radio-nuclide | /kg | /kg | /L | /kg |

TIME #####

- 30 Intake ends after (yr)
 70 Dose calc. ends after (yr)
 1 Release ends after (yr)
 0 No. of years of air deposition prior to the intake period

0 No. of years of irrigation water deposition prior to the intake period

FAR-FIELD SCENARIOS (IF POPULATION DOSE) #####

0 Definition option: 1-Use population grid in file POP.IN

0 2-Use total entered on this line

NEAR-FIELD SCENARIOS #####

Prior to the beginning of the intake period: (yr)

0 When was the inventory disposed? (Package degradation starts)

0 When was LOIC? (Biotic transport starts)

0 Fraction of roots in upper soil (top 15 cm)

0 Fraction of roots in deep soil

0 Manual redistribution: deep soil/surface soil dilution factor

0 Source area for external dose modification factor (m2)

TRANSPORT #####

====AIR TRANSPORT=====SECTION 1=====

| | | | |
|---|------------------------------------|---|-------------------------|
| 0 | 0-Calculat PM | 0 | Release type (0-3) |
| 1 | Option: 1-Use chi/Q or PM value | F | Stack release (T/F) |
| | 2-Select MI dist & dir | 0 | Stack height (m) |
| | 3-Specify MI dist & dir | 0 | Stack flow (m3/sec) |
| 0 | Chi/Q or PM value | 0 | Stack radius (m) |
| 0 | MI sector index (1=S) | 0 | Effluent temp. (C) |
| 0 | MI distance from release point (m) | 0 | Building x-section (m2) |
| T | Use jf data, (T/F) else chi/Q grid | 0 | Building height (m) |

====SURFACE WATER TRANSPORT=====SECTION 2=====

0 Mixing ratio model: 0-use value, 1-river, 2-lake

1.0 Mixing ratio, dimensionless

3400.0 Average river flow rate for: MIXFLG=0 (m3/s), MIXFLG=1,2 (m/s),

0 Transit time to irrigation withdrawal location (hr)

If mixing ratio model > 0:

0 Rate of effluent discharge to receiving water body (m3/s)

0 Longshore distance from release point to usage location (m)

0 Offshore distance to the water intake (m)

0 Average water depth in surface water body (m)

0 Average river width (m), MIXFLG=1 only

0 Depth of effluent discharge point to surface water (m), lake only

====WASTE FORM AVAILABILITY=====SECTION 3=====

0 Waste form/package half life, (yr)

0 Waste thickness, (m)

0 Depth of soil overburden, m

====BIOTIC TRANSPORT OF BURIED SOURCE=====SECTION 4=====

T Consider during inventory decay/buildup period (T/F)?

T Consider during intake period (T/F)?

0 Pre-Intake site condition.....

1-Arid non agricultural
2-Humid non agricultural
3-Agricultural

EXPOSURE #####

====EXTERNAL EXPOSURE=====SECTION 5=====

| | | | |
|--------|--|------|--------------------------|
| | Exposure time: | | Residential irrigation: |
| 0 | Plume (hr) | T | Consider: (T/F) |
| 4380.0 | Soil contamination (hr) | 2 | Source: 1-ground water |
| 100.0 | Swimming (hr) | | 2-surface water |
| 100.0 | Boating (hr) | 40.0 | Application rate (in/yr) |
| 500.0 | Shoreline activities (hr) | 6.0 | Duration (mo/yr) |
| 1 | Shoreline type: (1-river, 2-lake, 3-ocean, 4-tidal basin) | | |
| 8.0 | Transit time for release to reach aquatic recreation (hr) | | |
| 0 | Average fraction of time submersed in acute cloud (hr/person hr) | | |

====INHALATION=====SECTION 6=====

| | | | |
|--------|---|----------------------------|-------------------------|
| 8766.0 | Hours of exposure to contamination per year | | |
| 1 | 0-No resus- | 1-Use Mass Loading | 2-Use Anspaugh model |
| .0001 | pension | Mass loading factor (g/m3) | Top soil available (cm) |

====INGESTION POPULATION=====SECTION 7=====

| | | | |
|------|---|--|--|
| 0 | Atmospheric production definition (select option): | | |
| 0 | 0-Use food-weighted chi/Q, (food-sec/m3), enter value on this | | |
| line | | | |
| | 1-Use population-weighted chi/Q | | |
| | 2-Use uniform production | | |
| | 3-Use chi/Q and production grids (PRODUCTION will be overridden) | | |
| 0 | Population ingesting aquatic foods, 0 defaults to total (person) | | |
| 0 | Population ingesting drinking water, 0 defaults to total (person) | | |
| F | Consider dose from food exported out of region (default=F) | | |

Note below: S* or Source: 0-none, 1-ground water, 2-surface water
3-Derived concentration entered above

==== AQUATIC FOODS / DRINKING WATER INGESTION=====SECTION 8=====

F Salt water? (default is fresh)

| USE ? | FOOD TYPE | TRAN- SIT hr | PROD- UCTION kg/yr | -CONSUMPTION- HOLDUP da | RATE kg/yr | DRINKING WATER | |
|----------|--------------|--------------------|--------------------------|-------------------------------|---------------|----------------|--------------------|
| T | FISH | 0.00 | 0.0E+00 | 1.00 | 40.0 | 2 | Source (see above) |
| T | MOLLUS | 0.00 | 0.0E+00 | 0.00 | 6.9 | T | Treatment? T/F |
| T | CRUSTA | 0.00 | 0.0E+00 | 0.00 | 6.9 | 1.0 | Holdup/transit(da) |
| T | PLANTS | 0.00 | 0.0E+00 | 0.00 | 6.9 | 730.0 | Consumption (L/yr) |

#####

DISTRIBUTION -- WHC-SD-EA-TA-001

Westinghouse Hanford Company

| | |
|---------------------|-------|
| M. R. Adams | H4-55 |
| J. W. Cammann | H4-14 |
| L. B. Collard | H4-14 |
| M. P. Connelly (5) | H4-56 |
| J. D. Davis (5) | H4-55 |
| H. L. Debban | X0-43 |
| L. P. Diediker | T1-30 |
| K. R. Fecht | H4-56 |
| E. A. Fredenburg | X6-65 |
| K. A. Gano (2) | X0-21 |
| J. M. Garcia | R3-12 |
| E. M. Greager | L6-60 |
| W. E. Green | H4-55 |
| M. C. Hagood | H4-55 |
| M. J. Hartman | H4-56 |
| G. S. Hunacek | X0-41 |
| R. Khaleel | H4-14 |
| N. W. Kline | H0-31 |
| A. J. Knepp | H4-56 |
| K. J. Koegler | H4-55 |
| M. J. Lauterbach | H4-55 |
| A. H. Lu | H0-36 |
| N. M. Naiknimbaikar | H4-55 |
| R. W. Oldham | H4-57 |
| M. G. Piepho | H0-34 |
| P. D. Rittman(5) | H4-14 |
| J. P. Schmidt | X0-41 |
| W. A. Skelly | H4-55 |
| J. C. Sonnichsen | H4-14 |
| D. W. Templeton | A6-55 |
| L. W. Vance | A6-55 |
| D. J. Watson (10) | X0-41 |
| C. D. Wittreich | H4-55 |
| J. G. Woolard | H4-55 |